DEVELOPMENT OF ITERATIVE THERMAL ASPERITY DETECTION AND CORRECTION ALGORITHM

THEERACHAT THONGKAM

A THESIS SUBMITTED IN PARTIAL FULFILLMENT
OF THE REQUIREMENT FOR THE DEGREE OF
MASTER OF ENGINEERING IN DATA STORAGE TECHNOLOGY
COLLEGE OF DATA STORAGE INNOVATION
KING MONGKUT'S INSTITUTE OF TECHNOLOGY LADKRABANG
2013

KMITL-2013-DS-M-001-06

หัวข้อวิทยานิพนธ์	การพัฒนาอัลกอริทึมในการตรวจหาและแก้ไขความขรุขระเชิงความร้อนแบบวนซ้ำ
นักศึกษา	นายธีระชาติ ทองคำ
รหัสนักศึกษา	51068922
ปริญญา	วิศวกรรมศาสตรมหาบัณฑิต
สาขาวิชา	เทคโนโลยีการบันทึกข้อมูล
พ.ศ.	2556
อาจารย์ผู้ควบคุมวิทยานิพนธ์	รองศาสตราจารย์ ดร.พรชัย ทรัพย์นิธิ

บทคัดย่อ

ความขรุขระเชิงความร้อน (TA : thermal asperity) ก่อให้เกิดปัญหาที่สำคัญในระบบการบันทึกข้อมูลแบบแนวตั้ง เพราะจะลดทอนสัญญาณอ่านกลับ รวมถึงการก่อให้เกิดข้อผิดพลาดออกมาในขั้นตอนการตรวจหาข้อมูล โดยระบบที่ไม่มีการตรวจหาและแก้ไข TA จะมีประสิทธิภาพที่ไม่สามารถยอมรับได้ ซึ่งขึ้นอยู่กับความรุนแรงของผลกระทบจาก TA วิทยานิพนธ์นี้ ศึกษาประสิทธิภาพของวิธีการลดผลกระทบของ TA แบบวนซ้ำ ซึ่งเป็นการทำงานร่วมกันของการลดผลกระทบจาก TA และอีควอไรเซชัน แบบเทอร์โบในช่องสัญญาณแบบผลตอบสนองบางส่วนที่ถูกเข้ารหัส โดยวิธีการลดผลกระทบของ TA แบบวนซ้ำจะอาศัยเทคนิคการหาค่าขีดเริ่มเปลี่ยน (Threshold based technique) และเทคนิคการปรับเส้นโค้งที่เหมาะสม (Least squares fitting technique) จากการทดลองพบว่าวิธีการลดผลกระทบของ TA แบบวนซ้ำทั้งสองแบบมีความซับซ้อนที่ใกล้เคียงกัน แต่วิธีที่ใช้เทคนิคการปรับเส้นโค้งที่เหมาะสมมีประสิทธิภาพดีกว่า ดังนั้นวิธีการลดผลกระทบของ TA แบบวนซ้ำที่ใช้เทคนิคการปรับเส้นโค้งที่เหมาะสมจึงควรนำมาใช้ในระบบการบันทึกข้อมูลแบบแนวตั้ง โดยเมื่อเปรียบเทียบกับระบบที่ไม่มี TA จะแตกต่างเพียง 1dB เท่านั้น และดีกว่าวิธีการเดิมมากกว่า 2dB

Thesis	Development of Iterative Thermal Asperity Detection and Correction Algorithm
Student	Mr.Theerachat Thongkam
Student ID	51068922
Degree	Master of Engineering
Program	Data Storage Technology and Application
Year	2013
Thesis Advisor	Assoc.Prof.Dr.Pornchai Supnithi

ABSTRACT

Thermal asperities (TAs) cause a critical problem in perpendicular recording systems because they can distort the read back signal to the extent of causing an error burst in data detection process. System performance without a TA detection and correction algorithm can be unacceptable, depending on how severe the TA effect is. This thesis investigates the performance of an iterative TA suppression method, which jointly performs TA suppression and turbo equalization on coded partial-response channels. Specifically, two iterative TA suppression methods are compared (i.e., one is based on a threshold-based technique, and the other is based on a least-squares (LS) fitting technique) in terms of bit-error rate performance and complexity. Results indicate that two methods have comparable complexity, but the method based on a LS fitting technique performs better than that based on a threshold-based technique. Thus, it is worth employing the iterative TA suppression method based on the LS fitting technique in perpendicular recording systems. At the bit error rate (BER) of 10^{-4}, the proposed code difference 1dB compared to system with no TA effect and better than conventional method more than 2dB

Acknowledgements

First of all, I would like to express my sincere thank to Assoc. Prof. Dr. Pornchai Supnithi and Assoc. Prof. Dr. Piya Kovintavewat for advice and encouragement while working on this thesis. I would like to express my gratitude to my boss, Mr.Charin Thongjantanam and Mr. Atthaphol Mahattano for being supportive of my educational achievement and professional advancement. Finally, I would like to specially thank my family for their motivation and encouragement during my study.

Mr.Theerachat Thongkam

Contents

Contents (Cont)

List of Tables

List of Figures

List of Figures (cont)

Chapter 1
Introduction

1.1 Introduction

Nowadays, recording in digital format is very popular. Because most of the information is in digital form (e.g., image files, movie files, data files, documents, etc.), the demand for high storage capacity devices is increasing rapidly. Hard disk drive (HDD) is considered to be a low-cost device with high storage capacity and high reliability when compared to other devices in terms of price per megabyte [1]. Current HDDs are intended to use not only for personal computers, but also for electronic consumers such as a smart television, a digital video camera, and a music player, and so on.

In the reading process of HDDs, the MR (Magneto-resistive) head is used to detect the changes in magnetic flux via magnetization patterns, resulting in a transient voltage pulse at the output of the head. Generally, the magnetic medium is not smooth (or roughness), resulting from a manufacturing process or dirt on the medium [2]. In addition, the fly height between the read head and the medium is currently less than 10 nm. Therefore, when the read head moves into contact with an asperity, it results in a transient voltage signal known as thermal asperity (TA) added to the readback signal. This causes the amplitude of the readback signal to suddenly jump from the baseline of the normal readback signal according to the TA signal [3].

In general, the TA signal has low frequency and has the maximum amplitude of approximately 2-3 times the maximum amplitude of the normal readback with a rise time of about 60-150 nano-seconds and a decay time of 1-5 micro-seconds [2]. Practically, the TA can easily cause an error burst in the data detection process beyond the capability of the error-correction code (ECC) that can handle [3]. Normally, when a TA is detected on a medium, the location around that TA will be marked so as to protect the write head writing data on that location. However, this process cannot be marked all locations that contain TA [4]. Therefore, the technique to detect and correct TA is essential in magnetic data recording system.

Recently, HDD uses an iterative decoding for data recovery process. In addition, we found that the iterative decoding system without a TA detection and correction algorithm cannot reduce the impact of TA [5]. Therefore, the TA is a crucial problem for HDD systems because it can deteriorate the overall system performance. Hence, the TA suppression technique in HDD is extremely important.

Consequently, this study focuses on examining the algorithms to reduce the impact of TA in a perpendicular magnetic recording channel by applying an iterative TA detection and correction technique [6].

1.2 Objectives

The major objective of this research was to examine and reduce the impact of the TA in magnetic recording systems. The study starts from a channel model for a basic HDD recording, the iterative channel model, the TA effect, the algorithm for detecting and suppressing the TA in perpendicular magnetic recording channels.

1.3 Outcomes and Expectation

This thesis investigates the performance of an iterative TA suppression method, which jointly performs TA suppression and turbo equalization on coded partial-response channels. Specifically, two iterative TA suppression methods are compared (i.e., one is based on a threshold-based technique, and the other is based on a least-squares (LS) fitting technique) in terms of bit-error rate performance and complexity. Expectation is to have worth employing the iterative TA suppression method based on the LS fitting technique in perpendicular recording systems.

1.4 Conceptual Framework

Recently, the magnetic recording system uses the iterative decoding to improve the encoding efficiency by jointly performing a soft-out Viterbi algorithm (SOVA) and a low-density parity check (LDPC) decoding. Thus, the inspiration to utilize the soft information at the end of the LDPC decoding circuit to deduct the TA effect would be used in this thesis.

1.5 Hypothesis

There is much information changing between a SOVA detector and a LDPC decoder in the iterative magnetic recording. The changing has been performed under a given iteration. The soft information would be used to calculate the soft decision value or the hard decision value. Therefore, the idea of this research is to use the soft decision and the hard decision to deduct the TA effect embedded in the readback signal.

1.6 Scope of the Study

The scope of this thesis begins with examining the perpendicular recording channel, the TA effect and model, and the development of the iterative TA detection and correction. Then, the performance of the proposed algorithm is investigated and compared with that of the conventional system, which performs TA suppression and iterative decoding separately. Finally, we summarize the results of this thesis.

Chapter 2
Theory and Literature Review

This chapter shall discuss about hard disk drive technology and its theories related to the read-back signal model, magnetic recording channel model, target and equalizer design, SOVA (Soft-Output Viterbi Algorithm), error correction code LDPC (Low Density Parity Check) and the effect of thermal asperity (TA) on the magnetic recording channel. The details are given as follow.

2.1 Hard Disk Drive History

Recording data on hard disk drive is based on the magnetic recording principle. The magnetic recording technology has been improved so that it can increase the storage capacity. This section will provide the history of the recording technology of hard disk drives and the structure of the recording system.

Figure 2.1 Hard disk drive IBM model 305 RAMAC [6]

2.1.1 Hard disk drive technology

In 1888, Oberlin Smith [1] had invented magnetic recording technology and then it was firstly shown by engineer, Mr.Valdemar Poulsen, in 1898 as known as Telegraphone. In 1956, the first hard disk drive was released in the name of IBM 305 RAMAC as shown in Fig. 2.1. It can record the data by 5 Megabytes on 50 recorded disks and each disk has 24 inches in diameter [6]. The capacity per area is 2 Kbits/in^2 (kilobits per square inch) and its cost per megabyte is equal to $10,000 US (U.S. dollars). Nowadays, the capacity of hard disk drive can be increased to 1 terabyte with areal density at 420 Gbits/in^2 (gigabits per square inch) while its cost per megabyte is only $0.0002 US [6].

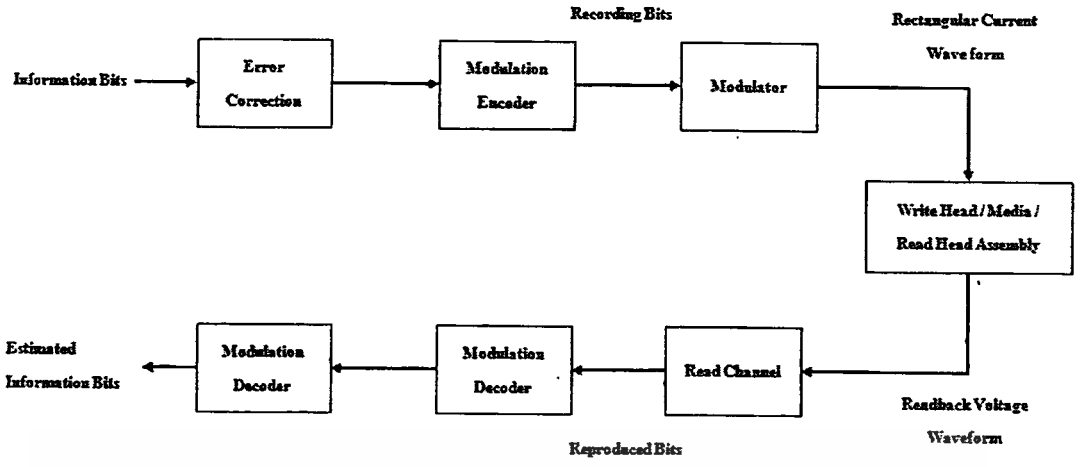

Figure 2.2 Data reading and writing of hard disk drive.

2.1.2 Reading and writing of hard disk drive

Reading and writing data on hard disk drive can be summarized in Fig. 2.2. Information bits are recorded by ECC such as RS (Read Solomon) code and LDPC (Low Density Parity Check) code which are popular and become the standard method. Then the data are encoded with modulation code such as RLL (Run Length Limited). Therefore, the data sequence is recorded by writing head on its recording media. At the read head, it could be detect the change of magnetic flux. At the position, magnetic flux and readable signal could be hand to the read channel in order to equalize it by equalizer and then detect its possibility bit order, before transplant to demodulation, and finally the output data of demodulation will be encoding with ECC for a require information bits.

The magnetic recording technology can be explained by using direction of magnetic north and south poles. Both are aligned with binary data of two states which are "0" and "1". At the beginning of recording, longitudinal direction of recording data is parallel to the magnetic recording medium as shown in Fig.2.3. However, there is some limitation for longitudinal magnetic recording since it has reached saturation point for increasing recording capacity. Consequently, the recording technology has been changed to perpendicular magnetic recording of which the direction of recording data is perpendicular to magnetic recording medium as shown in Fig. 2.4. Moreover, the perpendicular magnetic recording can increase the capacity up to 1 Tbit/in^2 by using the discrete track perpendicular magnetic recording. [8]

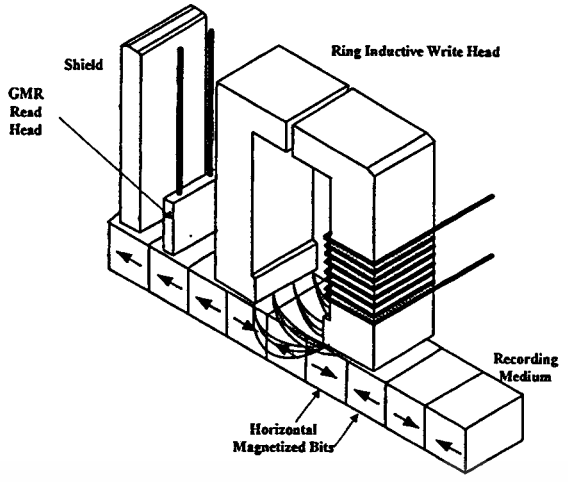

Figure 2.3 Longitude magnetic recording.

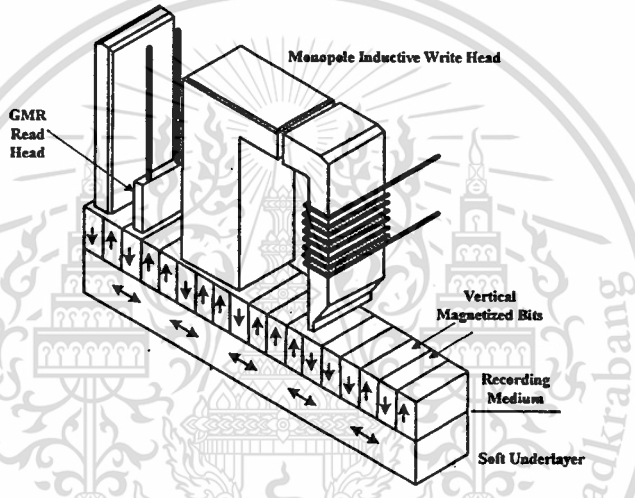

Figure 2.4 Perpendicular magnetic recording.

2.2 Read-Back Signal

This part shall discuss about readback signal model from output of read head which is magneto resistive (MR). When the read head moves to the position where there has a change of magnetic property on the recording media, read head will generate transition pulse as known as transition response $g(t)$ or $-g(t)$ corresponding to direction of the magnetic property. For longitudinal magnetic recording, transition pulse or Lorentzian pulse can be written as [8]

$$g(t) = \frac{1}{1+\left(\frac{2t}{\mathrm{PW}_{50}}\right)^2} \quad (2\text{-}1) \qquad (2\text{-}1)$$

where PW_{50} is the width of the pulse $g(t)$ at the location where the pulse amplitude is at the half of the height of the maximum amplitude. For the perpendicular magnetic recording, pulse transition can be written as [8]

$$g(t) = \text{erf}\left(\frac{2t\sqrt{\ln 2}}{PW_{50}}\right) \tag{2-2}$$

where erf (.) is the error defined by $\text{erf}(x) = \frac{2}{\sqrt{\pi}}\int_0^x e^{-t^2}dt$, PW_{50} is the width of the pulse $g'(t)$ or differential signal $g(t)$ at the position signal with amplitude and a half of the height of the maximum amplitude.

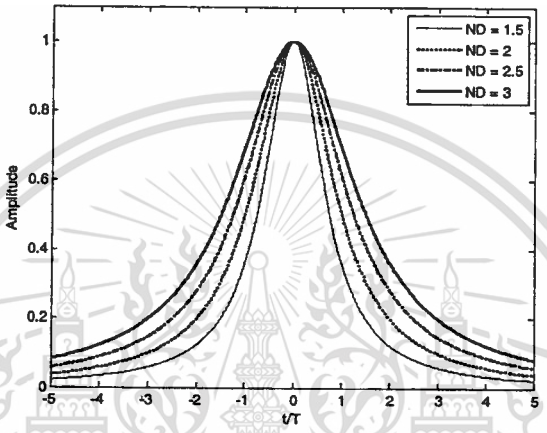

Figure 2.5 Transition pulse response of longitude magnetic recording.

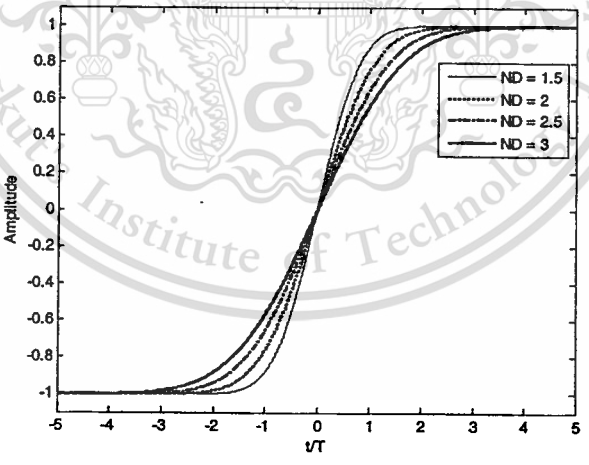

Figure 2.6 Transition pulse response of perpendicular magnetic recording.

In the context of magnetic recording, a normalized recording density (ND) is the density of data recording defined by

$$ND = \frac{PW_{50}}{T} \tag{2-3}$$

where T is the period of one data bit or bit cell. Practically, ND can indicate how many bits of data that PW_{50} area can record. If T is a constant value and the ND or PW_{50} is increased, a hard disk drive can hold more data. Fig. 2.5 shows the pulse response of the transition state for the longitude magnetic recording that is calculated from equation (2-1) and Fig. 2.6 shows the pulse response of perpendicular magnetic recording that is calculated from equation (2-2) at the level of the ND from the Fig. 2.5, it can be seen that the pulse transition covers many bit cells. As the ND is increased, the inter-symbol interference (ISI) is more severe because the pulse transition near the overlap tends to be higher. The relation between ND and PW_{50} is aligned with the equation (2-3).

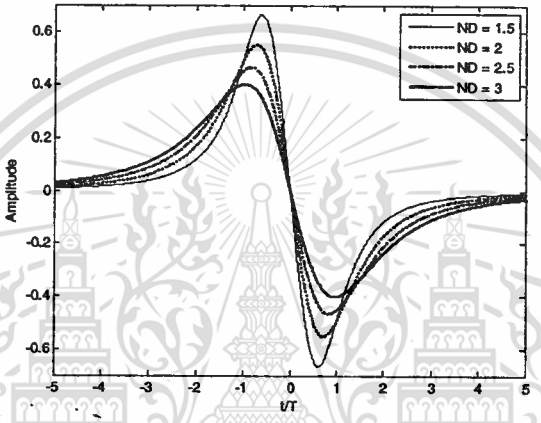

Figure 2.7 Dibit response of longitudinal magnetic recording.

As the signal of dibit pulse or the dibit response occurs when the reading head located to the areas where transition position occurs twice, it would make the value of net pulse becomes

$$m(t) = g(t) - g(t-T) \tag{2-4}$$

where $m(t)$ is the response as shown in Fig. 2.7. The frequency response of the response bits can be obtained by the continuous-time Fourier transform. The frequency response of a bit of a longitude magnetic recording is shown in Fig. 2.8 and can be written as [1], [6].

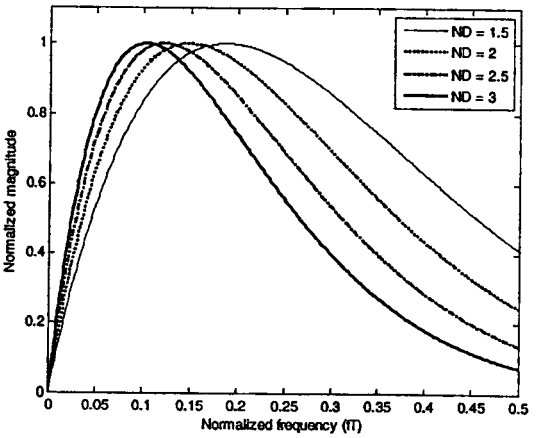

Figure 2.8 Frequency response of dibit pulse in longitudinal magnetic recording.

$$M(\Omega) = \exp\{-\pi |\Omega| ND\}\left(1-\exp\{-j2\pi\Omega\}\right) \tag{2-5}$$

where exp{.} is the exponential function and $j = \sqrt{-1}$ is the imaginary unit.

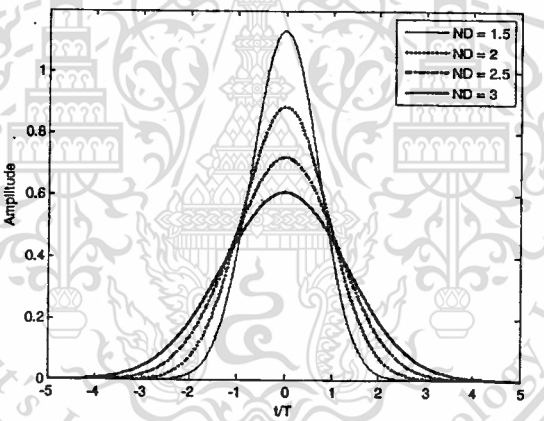

Figure 2.9 Dibit response of perpendicular magnetic recording.

The frequency response of $m(t)$ is shown in Fig. 2.9. The frequency response of of the dibit response in the perpendicular magnetic recording is shown in Fig. 2.10. It is which could be referred to [1],[6]

$$M(\Omega) = \frac{T}{j\pi\Omega}\exp\left\{-\frac{\pi^2\Omega^2 ND^2}{\ln(16)}\right\}\left(1-\exp\{-j2\pi\Omega\}\right) \tag{2-6}$$

where $\Omega = fT$ is normalized frequency, f = frequency (hertz), $|x|$ = absolute value of x and ln(.) is the natural logarithm.

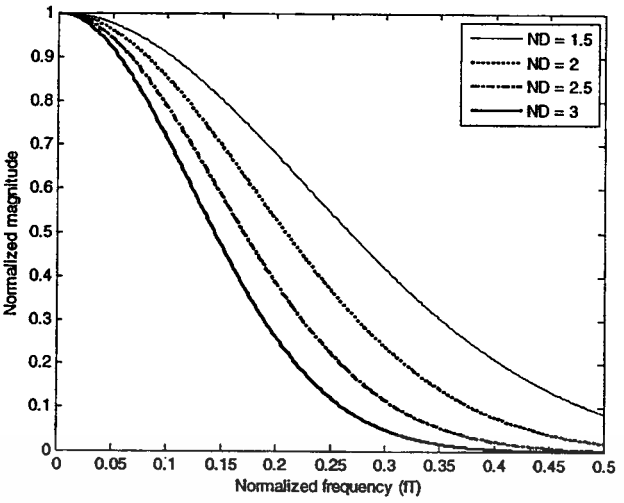

Figure 2.10 Frequency response of dibit pulse in perpendicular magnetic recording.

For longitudinal recording, partial response (PR) target, which has the coefficient of the target tab, is an integer. The equation of PR target in longitude magnetic recording has the form of

$$H(D) = (1-D)(1+D)^n \tag{2-7}$$

where $H(D)$ is recording target, D is delay operator and n is the integer. Fig. 2.11 shows the longitude magnetic recording PR target frequency response.

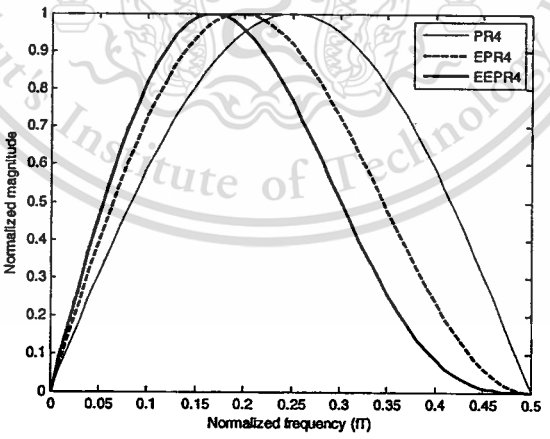

Figure 2.11 Frequency response of the PR target for longitudinal recording.

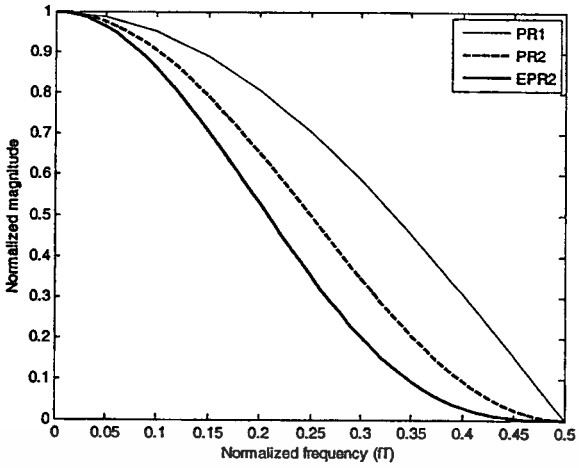

Figure 2.12 Frequency response of the PR target for perpendicular magnetic recording.

The partial response (PR) target of perpendicular recording is written in the form of

$$H(D) = (1+D)^n \tag{2-8}$$

There was direct current component in the perpendicular magnetic recording. So, there is no *D-1* as shown in Fig. 2.12. Anyway, the PR target of both longitude and perpendicular has been shown in Table 2-1.

Table 2-1 PR targets.

PR target	$n = 1$	$n = 2$	$n = 3$
Perpendicular Recording	PR1 [1 1] $H(D) = 1+D$	PR2 [1 2 1] $H(D) = (1+2D+D^2)$	EPR2 [1 3 3 1] $H(D) = (1+3D+3D^2+D^3)$
Longitude Recording	PR4 [1 0 -1] $H(D) = 1-D^2$	EPR4 [1 1 -1 -1] $H(D) = (1+D-D^2-D^3)$	EEPR4 [1 2 0 -2 -1] $H(D) = (1+2D-2D^3-D^4)$

Fig. 2.11 shows frequency response of each target for longitude recording and Fig. 2.12 shows the same for the perpendicular. Besides, there was the generalized partial response target (GPR) [9] which an integer would be the absolute number. GPR target could be designed by following the topic 2.4.2. Anyway, overall performance of GPR was better than PR when using the effective target which means using the same number of target's tab. [11]

2.3 Channel model of magnetic recording

Typical magnetic recording channel can be divided in two types. They are realistic channel model and ideal channel model. Realistic channel model is almost similar to the system of the hard disk drive because it includes all the essential elements that exist in read channel architecture of the hard disk drive. While the ideal channel model is often used in the study and analysis of the basic operation of signal processing systems. The system is not complex and easy to understand. In this thesis, we will explain only the realistic magnetic recording channel model, the uncoded system and iterative coded system.

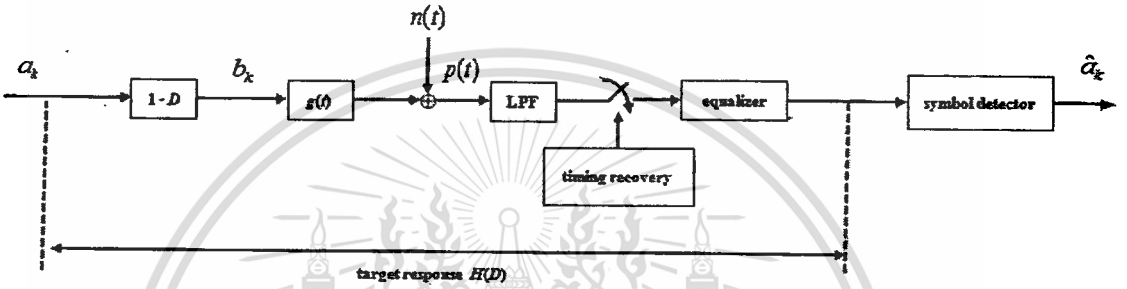

Figure 2.13 Uncoded realistic channel model.

2.3.1 Uncoded realistic magnetic recording channel model

Uncoded realistic magnetic recording channel model is explained in Fig. 2.16 which is a basic coding system. By the start of the data input binary sequence, $a_k \in \{0, 1\}$ with a bit period = T is passed to the circuit for a ideal differentiator or (1 - D), where D is the delay operator of T seconds. This process results in the transition data sequence $b_k \in \{0, \pm 1\}$ when ± 1 refers to positive transition or a negative transition and $b_k = 0$ is no change. The data b_k is modulated with the pulse signal change $g(t)$ in equation (2-1) for longitudinal magnetic recording system and equation (2-2) for perpendicular magnetic recording system. The readback signal $p(t)$ is disturbed by the additive white Gaussian noise (AWGN) $n(t)$ with the power spectrum density (PSD) of $N_0/2$ (W/Hz) and it can be written as

$$p(t) = \sum_k b_k g(t - kT) + n(t) \qquad (2\text{-}9)$$

On the receive side, the received signal $p(t)$ is filtered by the 7th-order Butterworth low-pass filter (LPF) circuit in order to eliminate the out-of-band noise, Then it would be sampled at the time point which is controlled by the timing recovery system. Sequence output of sampling circuit is passed to an equalizer and a check for the symbol detector in order to find the data input which the most likely

input sequence to determine is a_k and denoted by $\hat{a}_k$

2.3.2 Iterative realistic magnetic recording channel model

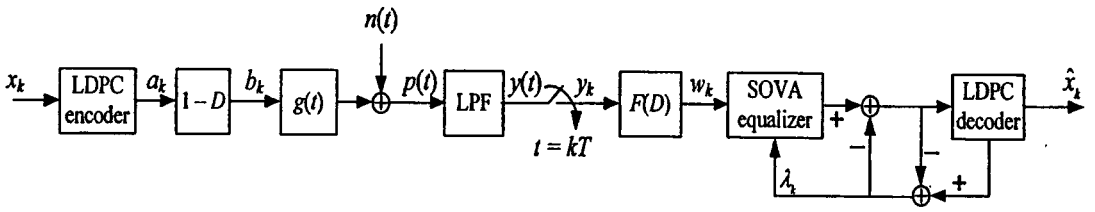

Figure 2.14 Iterative realistic magnetic recording channel model.

Currently, the data recording of new generation in hard disk drive utilizes an iterative decoding technology. Therefore, this thesis would pay attention to the iterative magnetic recording channel model with iterative decoding technique. This technique [10] uses soft-output Viterbi algorithm (SOVA) [10-12] (the principle of the algorithm SOVA described in section 2.5) to a LDPC decoder [10, 13] (the work of the LDPC code is described in section 2.6) for the operating system as shown in Fig. 2.14, when binary input sequence $x_k \in \{0, 1\}$, is encoded by the LDPC code. It results in data sequence $a_k \in \{0, 1\}$ and transfers to ideal differential $1 - D$ where, D is a delay operator T unit. This can result in transition data sequence $b_k \in \{0, \pm 1\}$, when ± 1 is positive transition or negative transition and $b_k = 0$, when there is no transition. Then read-back signal $p(t)$ can be written as

$$p(t) = \sum_k b_k g(t - kT) + n(t) \qquad (2\text{-}10)$$

At the receiver, the read-back signal $p(t)$ is passed through the 7th-order Butterworth low-pass filter (LPF) then the signal at the output of the low pass filter $y(t)$ would do a sampling at the time point $t = kT$ and results in data sequence y_k that assume no synchronization errors. The data are then sent to the equalizer circuit to adjust the shape of the signal according to the target to w_k and is sent to soft-output Viterbi algorithm (SOVA) and LDPC decoder. Data would exchange between the SOVA circuit and the LDPC circuit. It means that the data from SOVA circuit would be sent to the LDPC decoder then the soft output λ_k is sent back to SOVA circuit again.

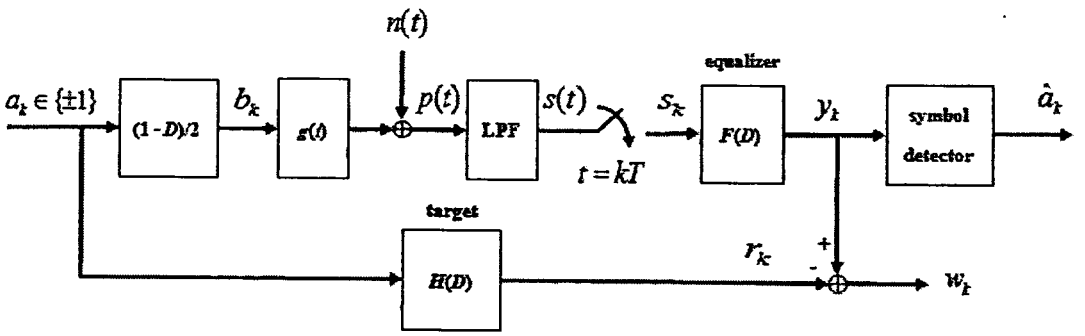

Figure 2.15 Magnetic recording channel model for target and equalizer designed.

2.4 Target and Equalizer Design

Equalizer and target design are very important for hard disk drive system. Equalizer functions by modification the signal to reach to target as much as possible and then transfers to the Viterbi circuit to find the most appropriate bit. This thesis would explain only the fixed target and equalizer constraint designs $h_0 = 1$ and the fixed target constraint [14-15]. In Fig. 2.15, where, w_k is the difference between the output sequence of equalizer $\{y_k\}$ and the output sequence of target $\{r_k\}$ which represent as $w_k = y_k - r_k$ and data sequence $y_k = s_k * f_k$, $r_k = a_k * h_k$, where, $F(D) = \sum_{k=-K}^{K} f_k D^k$ is the equalizer which has a total number of tap of $N = 2K+1$ and $H(D) = \sum_{k=0}^{L} h_k D^k$ is the target when

$$E\left[w_k^2\right] = E\left[\left(y_k - r_k\right)^2\right]$$
$$= E\left[\left(s_k * f_k - a_k * h_k\right)^2\right] \quad (2\text{-}11)$$

where * is the convolution operator, f_k is the absolute number of k of equalizer, h_k is the absolute number of k of target. Equation (2-12) can be written in the matrix form as

$$E\left[w_k^2\right] = E\left[\left(\mathbf{s}^T\mathbf{f} - \mathbf{a}^T\mathbf{h}\right)^2\right] \quad (2\text{-}12)$$

where $\mathbf{f} = [f_{-K}..f_0..f_K]^T$ is vector column of equalizer when $N = 2K+1$. Equalizer length, $\mathbf{s} = [s_{k+K}...s_k...s_{k-K}]^T$ is a vector column of read-back and also $\mathbf{a} = [a_k\ a_{k-1}\ ...\ a_{k-L-1}]^T$ is a vector column of input sequence. Let $\mathbf{R}$ = auto-correlation matrix of size $N \times N$ of data sequence s_k, $\mathbf{P}$ = cross-correlation matrix of size $N \times L$ of data sequence s_k and a_k, $\mathbf{U}$ = auto-correlation matrix of size $L \times L$ of data sequence a_k all these variables can be written as following equations;

$$\mathbf{R}(i,j) = E\left[\sum_{k=0}^{S-1} s_{k+K-i} s_{k+K-j}\right], \text{ when } -K \le i,j \le K \quad (2\text{-}13)$$

$$\mathbf{U}(i,j) = E\left[\sum_{k=0}^{S-1} a_{k-i} a_{k-j}\right], \text{ when } 0 \le i,j \le L-1 \quad (2\text{-}14)$$

$$\mathbf{P}(i,j) = E\left[\sum_{k=0}^{S-1} s_{k+K-i} a_{k-j}\right], \text{ when } -K \le i \le K, 0 \le j \le L-1 \quad (2\text{-}15)$$

where S = the length of input sequence a_k, and $E[.]$ = expectation operator. When we replace the equation (2-13), (2-14) and (2-15) in the equation (2-12), we would have a new equation as

$$E\left[w_k^2\right] = \mathbf{f}^T\mathbf{R}\mathbf{f} - 2\mathbf{f}^T\mathbf{P}\mathbf{h} + \mathbf{h}^T\mathbf{U}\mathbf{h} \quad (2\text{-}16)$$

In order to prevent f = 0 and h = 0, we have to add a fixed constraint into the process to target the minimum value of $E\left[w_k^2\right]$.

2.4.1 Monic constraint (h_0 =1)

We use h_0 = 1 for the co-efficient number of the first tap of target. If perpendicular vector **I**, size $L \times 1$, which the first member of the group equals to 1 and the other members of the group equal to 0, which was $\mathbf{I} = [1, 0, 0, \ldots, 0]^T$ the constraint a new field can be written in the form of a matrix is $\mathbf{I}^T\mathbf{h} = 1$. The target and equalizer design by this method depends on the principle of minimization of the mean square error in the equation (2-11) and try to keep the value of $\mathbf{I}^T\mathbf{h} = 1$ all the time, it can be written as following equation.

$$E\left[w_k^2\right] = \mathbf{f}^T\mathbf{R}\mathbf{f} - 2\mathbf{f}^T\mathbf{P}\mathbf{h} + \mathbf{h}^T\mathbf{U}\mathbf{h} - 2\lambda\left(\mathbf{I}^T\mathbf{h} - 1\right) \quad (2\text{-}17)$$

By minimization of the value of equation (2-16) and λ is a Lagrange multiplier. The equation (2-17) has a minimum value which can be achieved by differentiation compared with **f**, **h** and λ respectively, and indicate the differentiation equation before solving the equations of equation (2-17) with respect to **f**, i.e.,

$$\frac{\partial E\left[w_k^2\right]}{\partial \mathbf{f}} = 2\mathbf{Rf} - 2\mathbf{Ph}$$

$$2\mathbf{Rf} - 2\mathbf{Ph} = 0$$

$$\mathbf{f} = \mathbf{R}^{-1}\mathbf{Ph} \tag{2-18}$$

Differentiation of equation (2-17) with respect to **h**, we would have

$$\frac{\partial E\left[w_k^2\right]}{\partial \mathbf{h}} = -2\mathbf{P}^{\mathrm{T}}\mathbf{f} + 2\mathbf{Uh} - 2\lambda\mathbf{I} \tag{2-19}$$

When we replace f in the equation (2-19), we would have

$$-\mathbf{P}^{\mathrm{T}}(\mathbf{R}^{-1}\mathbf{Ph}) + \mathbf{Uh} = \lambda\mathbf{I}$$

$$\mathbf{h} = \lambda\left(\mathbf{U} - \mathbf{P}^{\mathrm{T}}\mathbf{R}^{-1}\mathbf{P}\right)^{-1}\mathbf{I}. \tag{2-20}$$

Differentiating equation (2-17) with respect to λ, we have

$$\frac{\partial E\left[w_k^2\right]}{\partial \lambda} = -2\mathbf{I}^{\mathrm{T}}\mathbf{h} + 2$$

$$-\mathbf{I}^{\mathrm{T}}\mathbf{h} + 1 = 0 \tag{2-21}$$

When we replace **h** in the equation (2-21), we have

$$\mathbf{I}^{\mathrm{T}}\lambda(-\mathbf{P}^{\mathrm{T}}\mathbf{R}^{-1}\mathbf{P} + \mathbf{U})^{-1}\mathbf{I} = 1$$

$$\lambda = \frac{1}{\mathbf{I}^{\mathrm{T}}\left(-\mathbf{P}^{\mathrm{T}}\mathbf{R}^{-1}\mathbf{P} + \mathbf{U}\right)^{-1}\mathbf{I}}. \tag{2-22}$$

So we would be able to calculate the target and equalizer value from the equation (2-22), (2-21) and (2-20), respectively.

2.4.2 Fixed target constraint

For the fixed target constraint, target is determined from the outset by Table 2-1, what is needed to design an equalizer **f** appropriate to the target that can be obtained from equation (2-18) which is

$$\mathbf{f} = \mathbf{R}^{-1}\mathbf{Ph} \tag{2-24}$$

This would guaranteed that MMSE value is equal to the value from the equation (2-24)

This design method is very useful because the chip of hard disk drive would be designed specifically for only one type of target.

There are several types of target and equalizer designs. Two of them are described in the Section 2.4.1 and 2.4.2. Other types of this design includes monic constraint (h_0=1) and constraint of ($\mathbf{h}^T\mathbf{h} = 1$)

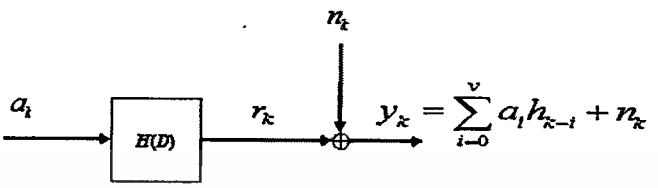

Figure 2.16 Channel model.

2.5 Soft-output Viterbi algorithm (SOVA)

Log-likelihood ratio (LLR) is an output from the algorithm of SOVA algorithm [10-12] or soft-output Viterbi algorithm which is similar to the BCJR (L. R. Bahl, J. Cocke, F. Jelinek, and J. Raviv) algorithm [10], [16]. It is different from Viterbi algorithm [1] because the output of Viterbi algorithm is the hard output which is 0 or 1 and this output would be ready to use. The SOVA algorithm has more advantages because it is less complex compared to BCJR algorithm. This would make it easier to be developed and be able to use in many applications which require an iterative decoding, also a decoding of hard disk drive. The differences between SOVA algorithm and Viterbi algorithm are as follow:

1. SOVA algorithm uses the modified branch metric which includes an effect of a priori probability of bit data.
2. SOVA algorithm gives the output as soft output which indicates the decision reliability of data in each bit.

From the channel model of signal in Fig. 2.16, the branch metric of Viterbi algorithm $\rho_k(u,q)$ is a transition from state u at time k to the state q at time k+1 in k(k-th state). This is shown in

$$\rho_k(u,q) = \ln\left(p(y_k \mid a_k)\right) = \ln\left(\frac{1}{\sqrt{2\pi\sigma^2}}\right) - \frac{1}{2\sigma^2}\mid y_k - \hat{r}(u,q)\mid^2 \qquad (2\text{-}25)$$

where $\hat{r}(u,q)$ is an output from the channel which is associated with the transition (u,q) as shown in trellis diagram and is a variant of AWGN interfering signal n_k

When we place a priori probability of bit data input a_k into the branch metric, so we would be able to rewrite the branch metric of SOVA algorithm as shown in equation below [10]

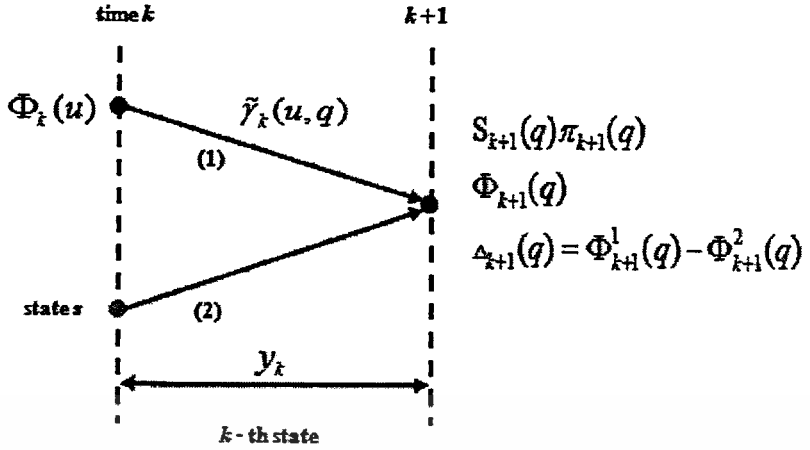

Figure 2.17 Trellis diagram of SOVA algorithm.

$$\tilde{\gamma}_k(u,q)=\ln\left(p(y_k;a_k)\right)=\ln\left(\frac{1}{\sqrt{2\pi\sigma^2}}\right)-\frac{1}{2\sigma^2}|y_k-\hat{r}(u,q)|^2+\frac{\hat{a}(u,q)\lambda_a(a_k)}{2} \quad (2\text{-}26)$$

where $p(y_k;a_k)=p(y_k|a_k)p(a_k),\hat{a}(u,q)$ is the input from a channel associated with the transition *(u,q)* and $\lambda_a(a_k)$ are priori probability of bit input a_k

The SOVA algorithm would search for the maximum or the highest path metric, when the path metric at the status of *q* at a time point of *k*+1 is equal to the sum of branch metric in the equation (2-26) which is

$$\Phi_{k+1}(q)=\sum_{i=0}^{k}\tilde{\gamma}_i \quad (2\text{-}27)$$

where $\tilde{\gamma}_i$ is the branch metric at a time point of *i* corresponding with survivor path at status *q* at a time point of *k*+1. SOVA algorithm has the similar pattern of work to the Viterbi algorithm in that it chooses the estimate value of input of a maximum path metric which we call maximum likelihood (ML) path. However, the SOVA algorithm uses a branch metric in the equation (2-26). Moreover, SOVA algorithm is able to calculate the value of LLR of each bit data when the LLR value indicates the reliability of the bits of information that should be worth something, and there is much more reliability.

To calculate the LLR of SOVA algorithm of each data bit, see Fig. 2.17, the trellis diagram at *k* metric path, at status *q*, at a time point of *k*+1 which is calculate from

$$\Phi_{k+1}(q)=\ln\left(p\left(\mathbf{y}_0^k;\mathbf{a}_0^k\right)\right) \quad (2\text{-}28)$$

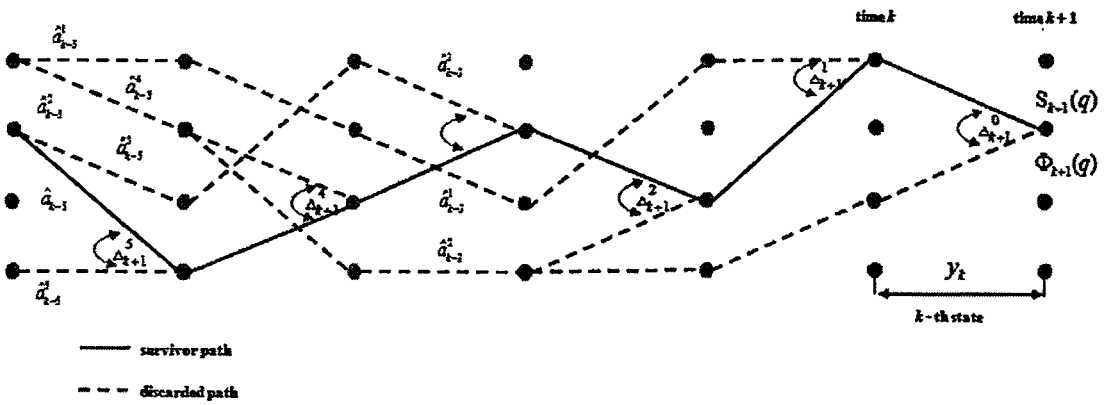

Figure 2.18 Trellis diagram with the difference of metric path and SOVA algorithm.

where $\mathbf{y}_0^k = [y_0, y_1, ..., y_k]$ is the data sequence which needs to be decoded from a time point of 0 to a time point of *k* and $\mathbf{a}_0^k = [a_0, \mathbf{a}_1, ..., \mathbf{a}_k]$ is the input sequence from a time point of 0 to a time point of *k* which is associated with $\mathbf{y}_0^k$ and

$$p\left(\mathbf{y}_0^k; \mathbf{a}_0^k\right) = e^{\Phi_{k+1}(q)} \tag{2-29}$$

The output of SOVA algorithm indicates the reliability of the decision of data bit from Fig. 2.17, we find that there are 2 transition paths that come to a status *q*, at the time point of *k*+1 that *is* (*u*,*q*) and (*s*,*q*) which has the magnetic path $\Phi^1_{k+1}(q)$ and $\Phi^2_{k+1}(q)$ respectively. If assumption is $\Phi^1_{k+1}(q) > \Phi^2_{k+1}(q)$ it means that the path (1) is the best transition path to a status *q* at the time point of *k*+1. So, the SOVA algorithm would choose path (1) as a part of survivor path at state *q*, at the time point of *k*+1, which is the definition of path metric difference is

$$\Delta_{k+1}(q) = \Phi^1_{k+1}(q) - \Phi^2_{k+1}(q) \tag{2-30}$$

It means that $\Delta_{k+1}(q) \geq 0$, so the probability of the correct decision is calculated from

$$\Pr[\text{correct decision at } \psi_{k+1} = q] = \frac{e^{\Phi^{(1)}_{k+1}(q)}}{e^{\Phi^{(1)}_{k+1}(q)} + e^{\Phi^{(2)}_{k+1}(q)}} = \frac{e^{\Delta_{k+1}(q)}}{1 + e^{\Delta_{k+1}(q)}}, \tag{2-31}$$

where Pr[*x*] = probability of *x* and LLR of the correct decision is equal to

$$\text{LLR} = \ln\left(\frac{\Pr[\text{correct decision at } \psi_{k+1} = q]}{1 - \Pr[\text{correct decision at } \psi_{k+1} = q]}\right) = \Delta_{k+1}(q) \tag{2-32}$$

It means that the combination of the difference of metric path from Viterbi algorithm is equal to LLR of the probability of the correct decision.

Practically, the Viterbi algorithm would be decided when its bit reaches at the time *k* as $\hat{a}_k$ then after the time pass δT where, δT is decoding depth and *T* is the bit time period which normally used $\delta \geq 5(v+1)$, *v* is the channel's memory at a time *k*. The Viterbi Algorithm would encode bit code at $k-\delta$ which $\hat{a}_{k-\delta}$ by consideration on Trellis diagram as in Fig. 2.18 for when there is the survivor path which shown in black thick line when it reaches *q* state at the time *k+1* is $\mathbf{S}_{k+1}(q)$ and the matrix's distance would be $\Phi_{k+1}(q)$. Moreover, the discarded path is still shown in Fig. 2.18 by dashed lines which are $\delta+1$ path. If we indicate Δ_k^d to be the differentiated between existing path and the discarded path at the time *k-d*, it would be called *d*-th path. In addition, if $\hat{a}_{k-\delta}$ is the input bit which is aligned with ML path at the time $k-\delta$ (or the input bit which Viterbi algorithm do the encoding at the time *k*) and $\hat{a}_{k-i}^d$ is the input bit which is aligned with the *d* path (discarded path) at the time *k-i*, when *i* is integer.

If the bit data $\hat{a}_{k-\delta}^d$ on the *d* path (discarded path) has the bit data $\hat{a}_{k-\delta}$ that shows the system would not have any error if the Viterbi chooses the discarded path to be the survivor path. So the traceability of the Viterbi decision would be infinity. However, if there is $\hat{a}_{k-\delta}^d \neq \hat{a}_{k-\delta}$ that shows the error would happen at the time $k-\delta$ in the *d* path (discarded path) which is defined by

$$\hat{e}_{k-\delta}^d = \hat{a}_{k-\delta} \oplus \hat{a}_{k-\delta}^d \tag{2-33}$$

where $\hat{a}_{k-\delta} \in \{\pm 1\}$, $\hat{a}_{k-\delta}^d \in \{\pm 1\}$,and $\oplus$ are the addition in binary field GF(2) (GF: Galois field) to be the addition identity which equal 1 as in following

$$1 \oplus 1 = 1,\ 1 \oplus -1 = -1,\ -1 \oplus 1 = -1,\ -1 \oplus -1 = 1 \tag{2-34}$$

Similar to the equation (2-32), the LLR of bit's error would equal Δ_k^d. So, if we combine these two cases together, we would have the LLR of data bit's error at the time $k-\delta$ on the d path (discard path) which equals

$$\lambda\left(\hat{e}_{k-\delta}^{d}\right)=\ln\left(\frac{p\left(\hat{e}_{k-\delta}^{d}=1\right)}{p\left(\hat{e}_{k-\delta}^{d}=-1\right)}\right)=\begin{cases}\infty, & \text{if } \hat{a}_{k-\delta}=\hat{a}_{k-\delta}^{d}\\ \Delta_k^d, & \text{if } \hat{a}_{k-\delta}\neq\hat{a}_{k-\delta}^{d}\end{cases} \tag{2-35}$$

Practically, each discarded path would leave evidence about the data bit's $\hat{a}_{k-\delta}$ traceability to make the correction encoding. So the possible of discard path which from combination of all error for the $\hat{a}_{k-\delta}$ could be calculated from

$$\hat{e}_{k-\delta}=\sum_{d=0}^{\delta}\oplus\hat{e}_{k-\delta}^{d}=\hat{e}_{k-\delta}^{0}\oplus\hat{e}_{k-\delta}^{1}\oplus\ldots\oplus\hat{e}_{k-\delta}^{\delta} \tag{2-36}$$

So, the LLR of the data bit $\hat{a}_{k-\delta}$ would be

$$\lambda\left(\hat{a}_{k-\delta}\right)=\hat{a}_{k-\delta}\lambda\left(\hat{e}_{k-\delta}\right)=\hat{a}_{k-\delta}\lambda\left(\sum_{d=0}^{\delta}\oplus\hat{e}_{k-\delta}^{d}\right) \tag{2-37}$$

where $\hat{a}_{k-\delta}\in\{\pm1\}$ is determine of sign of LLR and $\lambda\left(\hat{e}_{k-\delta}\right)\geq 0$ is the determine of reliability of $\hat{a}_{k-\delta}$

2.6 LDPC code

LDPC code (low-density parity check) has been considered as a type of linear code and accepted that it is the best of error correction code (ECC) because its performance almost reaches the Shannon limit. This section explains a linear block code and an LDPC code.

2.6.1 Linear block code

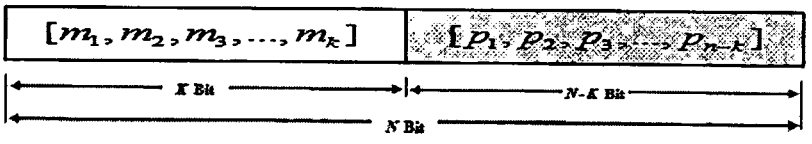

Figure 2.19 Linear Block Code Structure.

The parameter for linear block code is (*N*, *K*), where *N* is the number of bits in a codeword, *K* is the number of message bits, and *N* - *K* is the number of redundant bits. Let $\mathbf{m} = [m_1, m_2, m_3, \ldots, m_K]$ be a vector of message bits, $\mathbf{c} = [c_1, c_2, c_3, \ldots, c_N]$ be a codeword vector, and $\mathbf{p} = [p_1, p_2, p_3, \ldots, p_{N-K}]$ be a vector of parity bits. Fig. 2.19 shows the (*n*, *k*) linear block code structure, and the code rate *R* is defined as

$$R = \frac{K}{N} \tag{2-38}$$

where $0 < R \leq 1$. Practically, the code rate should be closed to 1 to reduce the number of parity bits. In general, the Hamming weight (w_H) could be used to indicate the performance of each linear blocking code. $w_H(c_i)$ is the number of bit 1's in c_i codeword, and Hamming distance d_H is the distance between the adjacent codewords defined by

$$d_H(c_i, c_{i+1}) = |w_H(c_i) - w_H(c_{i+1})| \tag{2-39}$$

where c_i and c_{i+1} are adjacent codeword. The minimum distance is the shortest Hamming distance d_{min}. Given d_{min}, the capability of correcting *t*-bit errors in each codeword would be calculated from

$$t = \frac{|d_{\min} - 1|}{2} \tag{2-40}$$

and it can detect an error of length

$$e = d_{\min} - 1 \tag{2-41}$$

The encoding of a linear block code can be performed by multiplying the message vector **m** with the *N*×*K* generator matrix **G** given by

$$\mathbf{G}_{N\times K} = \left[\mathbf{I}_{K\times K} \middle| \mathbf{P}_{K\times(N-K)}\right] = \begin{bmatrix} 1 & 0 & \cdots & 0 & p_{1,1} & p_{1,2} & \cdots & p_{1,(n-k)} \\ 0 & 1 & \cdots & 0 & p_{2,1} & p_{2,2} & \cdots & p_{2,(N-K)} \\ \vdots & \vdots & \ddots & \vdots & \vdots & \vdots & \ddots & \vdots \\ 0 & 0 & \cdots & 1 & p_{K,1} & p_{K,2} & \cdots & p_{K,(N-K)} \end{bmatrix} \tag{2-42}$$

where $\mathbf{I}_{K\times K}$ is an $K\times K$ identity matrix and P is a $K\times(N\text{-}K)$ parity matrix. The multiplication between m and G gives a codeword c according to

$$\mathbf{c} = \mathbf{mG} = [m_1, m_2, m_3, \ldots, m_K \; p_1, p_2, p_3, \ldots, p_{N-K}] \qquad (2\text{-}43)$$

Because the message bits are totally separate from the parity bits, this characteristic of the code is called a systematic code. In general, the linear block code would be indicated by a $(N\text{-}K)\times N$ parity check matrix H, where the relationship between G and H is given by

$$\mathbf{HG}^T = 0 \qquad (2\text{-}44)$$

In any codeword, it could be always explained by $\mathbf{Hc}^T = \mathbf{HG}^T\mathbf{m}^T = 0$ where H is expressed as

$$\mathbf{H}_{(N-K)\times N} = \left[\mathbf{P}^T \middle| \mathbf{I}_{(N-K)\times(N-K)}\right] \qquad (2\text{-}45)$$

Practically, syndrome decoding is used for decoding a linear block code, where s is the syndrome vector defined by

$$\mathbf{s} = \mathbf{Hr}^T, \qquad (2\text{-}46)$$

where $\mathbf{r} = \mathbf{c} \oplus \mathbf{e} = [r_1, r_2, r_3, \ldots, r_N]$ is a vector of received data, $\oplus$ is a modulo operator, $\mathbf{e} = [c_1, c_2, c_3, \ldots, c_N]$ is an error vector, and $e_i \in \{0, 1\}$. If $e_i = 1$, there would be an error in the i–th bit codeword. When we place $\mathbf{r} = \mathbf{c} \oplus \mathbf{e}$ into equation (2-46), it would be

$$\mathbf{s} = \mathbf{H}(\mathbf{c} \oplus \mathbf{e})^T = \mathbf{Hc}^T \oplus \mathbf{He}^T = \mathbf{He}^T \qquad (2\text{-}47)$$

It was found that the syndrome is based on the error. In general, if r has no error, the syndrome value would be equal to a zero vector. Additionally, the look-up table that shows the relationship between a syndrome vector and an error vector will help decode a linear block code. Finding the vector syndrome s from the codeword c, and then use it to find an error vector e from the look-up table. Finally, the decoded codeword is obtained from

$$\hat{\mathbf{c}} = \mathbf{r} + \mathbf{e} \qquad (2\text{-}48)$$

where $\hat{\mathbf{c}}$ is the estimated codeword.

2.6.2 LDPC code

Suppose a message sequence that we would like to encode is $\mathbf{m} = [m_1, m_2, m_3,..., m_K]$ with K bit, and a codeword of N bit is $\mathbf{c} = [c_1, c_2, c_3,..., c_N]$, whose structure is given by

$$\mathbf{c} = [\mathbf{m} \mid \mathbf{p}] = [m_1, m_2, m_3,..., m_K \mid p_1, p_2, p_3,..., p_{N-K}] \qquad (2\text{-}49)$$

where $\mathbf{p}$ is a parity vector of $(N - K)$ bits. Generally, LDPC code would be indicated by an $M \times N$ parity check matrix $\mathbf{H}$, where $M = N - K$. The codeword $\mathbf{c}$ must satisfy the following condition

$$\mathbf{H}\mathbf{c}^{\mathrm{T}} = 0_{M\times 1} \qquad (2\text{-}50)$$

where $0_{M\times 1}$ is a $M \times 1$ zero vector. If the $\mathbf{H}$ matrix is of the form

$$\mathbf{H} = [\mathbf{H}_1 \mid \mathbf{H}_2], \qquad (2\text{-}51)$$

where $\mathbf{H}_1$ has $M \times K$ dimension and $\mathbf{H}_2$ has $M \times (N\text{-}K)$ dimension. Therefore, when we replace the equation (2-49) and (2-51) in (2-50), it would be

$$[\mathbf{H}_1 \ \mathbf{H}_2]\begin{bmatrix}\mathbf{m}^{\mathrm{T}} \\ \mathbf{p}^{\mathrm{T}}\end{bmatrix} = 0 \qquad (2\text{-}52)$$

$$\mathbf{H}_1\mathbf{m}^{\mathrm{T}} + \mathbf{H}_2\mathbf{p}^{\mathrm{T}} = 0 \qquad (2\text{-}53)$$

$$\mathbf{p}^{\mathrm{T}} = (\mathbf{H}_2)^{-1}\mathbf{H}_1\mathbf{m}^{\mathrm{T}} \qquad (2\text{-}54)$$

Basically, the LDPC code can be decoded by a message passing algorithm (MPA), which can be easily performed by using a Tanner graph [27, 28].

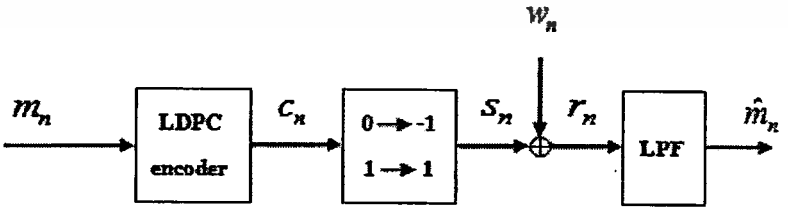

Figure 2.20 AWGN channel which encode by LDPC code.

Consider an AWGN channel with LDPC coding in Fig. 2.20. The input data $m_n \in \{0, 1\}$ with K bits is encoded by a regular (j, k) LDPC code to obtain a sequence $c_n \in \{0, 1\}$ with N bits. Then, the sequence c_n is mapped to a sequence $s_n \in \{\pm 1\}$. The

received sequence can be written as

$$r_n = s_n + w_n \tag{2-55}$$

where $s_n = 2c_n - 1$ is a channel output, w_n is an additive white Gaussian noise (AWGN) with zero mean and variance σ^2.

Only a systematic code would be explained in this topic. Let $\mathbf{m} = [m_1, m_2, m_3, \ldots, m_K]$ be a message vector, $\mathbf{c} = [c_1, c_2, c_3, \ldots, c_N]$ be a codeword vector, and $\mathbf{r} = [r_1, r_2, r_3, \ldots, r_N]$ be a received vector. To make decision, we choose $\mathbf{c}$ to be the maximum *a posteriori* (MAP), which would make the a posteriori probability (APP) $\Pr[c_n = c|\mathbf{r}]$ to have the maximum value in each n time. The MAP would calculate the log-likelihood ratio (LLR) in APP λ_n from

$$\lambda_n = \log\left(\frac{\Pr[c_n = 1|\mathbf{r}]}{\Pr[c_n = 0|\mathbf{r}]}\right) = \log\left(\frac{\Pr[c_n = 1|r_n;\mathbf{r}_{i\neq n}]}{\Pr[c_n = 0|r_n;\mathbf{r}_{i\neq n}]}\right) \tag{2-56}$$

Then, making the decision that $\hat{c}_n = 1$ when $\lambda_n \geq 0$ and $\hat{c}_n = 0$ when $\lambda_n < 0$, where $\mathbf{r}_{i\neq n}$ is the receiver vector exempt $i = n$. Based on Bey's law, equation (2-56) would be rewritten to

$$\begin{aligned}\Pr[c_n = 1|r_n;\mathbf{r}_{i\neq n}] &= \frac{p(r_n;c_n = 1;\mathbf{r}_{i\neq n})}{p(r_n;\mathbf{r}_{i\neq n})} \\ &= \frac{p(r_n|c_n = 1;\mathbf{r}_{i\neq n})\Pr(c_n = 1;\mathbf{r}_{i\neq n})}{p(r_n|\mathbf{r}_{i\neq n})p(\mathbf{r}_{i\neq n})} \\ &= \frac{p(r_n|c_n = 1)\Pr[c_n = 1|\mathbf{r}_{i\neq n}]}{p(r_n|\mathbf{r}_{i\neq n})}\end{aligned} \tag{2-57}$$

where $p(r_n|c_n = c)$ is a condition probability density function of r_n when $c_n = c \in \{0, 1\}$. Similarly, we obtain

$$\Pr[c_n = 0|r_n;\mathbf{r}_{i\neq n}] = \frac{p(r_n|c_n = 0)\Pr[c_n = 0|\mathbf{r}_{i\neq n}]}{p(r_n|\mathbf{r}_{i\neq n})} \tag{2-58}$$

Substituting equation (2-57) and equation (2-58) into equation (2-56), we obtain

$$\lambda_i = \log\left(\frac{p(r_n \mid c_n = 1)\Pr[c_n = 1 \mid \mathbf{r}_{i \neq n}]}{p(r_i \mid c_n = 0)\Pr[c_n = 0 \mid \mathbf{r}_{i \neq n}]}\right)$$
$$= \log\left(\frac{p(r_n \mid c_n = 1)}{p(r_n \mid c_n = 0)}\right) + \log\left(\frac{\Pr[c_n = 1 \mid \mathbf{r}_{i \neq n}]}{\Pr[c_n = 0 \mid \mathbf{r}_{i \neq n}]}\right)$$
$$= \frac{2}{\sigma^2} r_n + \log\left(\frac{\Pr[c_n = 1 \mid \mathbf{r}_{i \neq n}]}{\Pr[c_n = 0 \mid \mathbf{r}_{i \neq n}]}\right) \quad (2\text{-}59)$$

where

$$p(r_n \mid c_n) = \frac{1}{\sqrt{2\pi\sigma^2}} \exp\left(\frac{-(r_n - 2c_n + 1)^2}{2\sigma^2}\right) \quad (2\text{-}60)$$

In equation (2-59), the first right term is intrinsic information, which comes from a received data r_n, a constant $2/\sigma^2$ is the channel reliability, and the second term of equation (2-59) is extrinsic information of c_n.

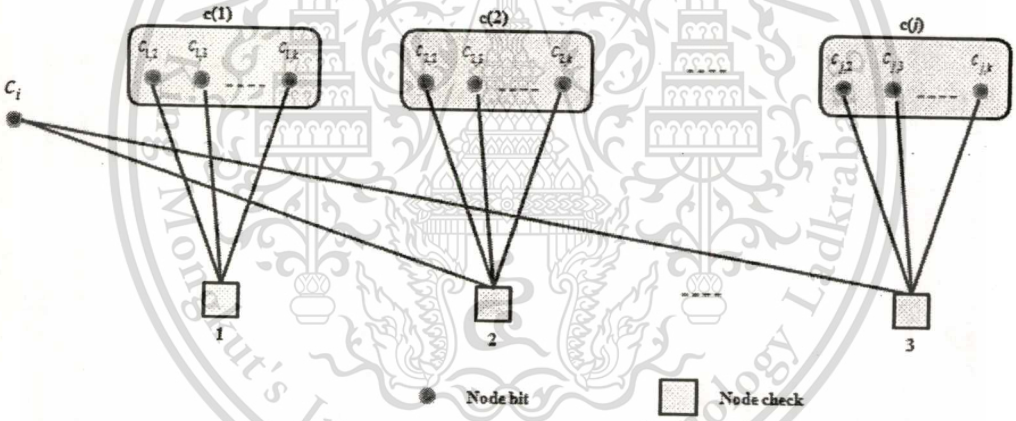

Figure 2.21 A Tanner graph of a regular (j, k) LDPC code.

Equation (2-56) could be arranged in the Tanner graph of a regular (j, k) LDPC as shown in Fig. 2.21. The n-th bit node connected to the j-th check node, and each node connects with others in$k - 1$ nodes. Let $\mathbf{c}(i) = [c_{i,2}, c_{i,3}, \ldots, c_{i,k}]$ be a set of $k - 1$ bit nodes (except the n-th bit node) that connects to the i-th check node when $i = [1, 2, \ldots, j]$. Fig. 2.21 shows that c_i depends on a parity value of $\mathbf{c}(1)$, $\mathbf{c}(2)$, ..., $\mathbf{c}(j)$ or $\Phi(\mathbf{c}(i))$ as follows

$$c_i = \begin{cases} 1, & \text{if } \Phi(c(1)) = \Phi(c(2)) = \ldots = \Phi(c(j)) = 1 \\ 0, & \text{if } \Phi(c(1)) = \Phi(c(2)) = \ldots = \Phi(c(j)) = 0 \end{cases} \quad (2\text{-}61)$$

2.6.3 Calculation the log-likelihood ratio (LLR) of data bit

Consider the $M \times N$ parity check matrix **H** of a regular (j, k) LDPC. From equation (2-61), the c_n data bit would be equal to the parity of $\mathbf{c}(i)$ vector as $c_n = \Phi(\mathbf{c}(i))$ for $i = \{1, 2, 3, \ldots, j\}$. Hence, the equation (2-56) could be rearranged as

$$\lambda_n = \frac{2}{\sigma^2} r_n + \log\left(\frac{\Pr\left[\Phi(\mathbf{c}(i)) = 1 \text{ for } i = 1,2,\ldots,j \mid r_{i\neq n}\right]}{\Pr\left[\Phi(\mathbf{c}(i)) = 0 \text{ for } i = 1,2,\ldots,j \mid r_{i\neq n}\right]}\right) \tag{2-62}$$

Given $r_{i\neq n}$, the $\mathbf{c}(1)$, $\mathbf{c}(2)$, . . ., $\mathbf{c}(j)$ would be conditionally free from each other. Then, the equation (2-62) could reduce to

$$\begin{aligned}\lambda_n &= \frac{2}{\sigma^2} r_n + \log\left(\frac{\prod_{i=1}^{j}\Pr\left[\Phi(\mathbf{c}(i)) = 1 \mid r_{i\neq n}\right]}{\prod_{i=1}^{j}\Pr\left[\Phi(\mathbf{c}(i)) = 0 \mid r_{i\neq n}\right]}\right) \\ &= \frac{2}{\sigma^2} r_n + \sum_{i=1}^{j}\log\left(\frac{\Pr\left[\Phi(\mathbf{c}(i)) = 1 \mid r_{i\neq n}\right]}{\Pr\left[\Phi(\mathbf{c}(i)) = 0 \mid r_{i\neq n}\right]}\right) \\ &= \frac{2}{\sigma^2} r_n + \sum_{i=1}^{j}\lambda_{\Phi(\mathbf{c}(i))}\end{aligned} \tag{2-63}$$

where $\lambda_{\Phi(\mathbf{c}(i))}$ is an LLR of $\Phi(\mathbf{c}(i))$. Because each bit is conditionally free from each other, the $\lambda_{\Phi(\mathbf{c}(i))}$ in each value will correspond to a hyperbolic tangent [10]. Therefore, if we let

$$\lambda_{i,l} = \log\left(\frac{\Pr\left[c_{i,l} = 1 \mid r_{i\neq n}\right]}{\Pr\left[c_{i,l} = 0 \mid r_{i\neq n}\right]}\right) \tag{2-64}$$

where $c_{i,l}$ is the l-th number of $\mathbf{c}(i)$ vector for $l = \{1, 2, \ldots, k\}$ by using the tangent hyperbolic, equation (2-64) could be rearranged to be [10]

$$\lambda_n = \frac{2}{\sigma^2} r_n - 2\sum_{i=1}^{j}\tanh^{-1}\left(\prod_{l=2}^{k}\tanh\left(\frac{-\lambda_{i,l}}{2}\right)\right) \tag{2-65}$$

or

$$\lambda_n = \frac{2}{\sigma^2} r_n - 2\sum_{i=1}^{j}\left\{\prod_{l=2}^{k} \text{sign}\left(-\lambda_{i,l}\right) \times f\left(\sum_{l=2}^{k}\left|\lambda_{i,l}\right|\right)\right\} \quad (2\text{-}66)$$

where $f(x) = -\log\left(\tanh\left(x/2\right)\right)$. In addition, to reduce the complexity of the algorithm, we could approximate the equation (2-66) as [10]

$$\lambda_n \approx \frac{2}{\sigma^2} r_n - 2\sum_{i=1}^{j}\left\{\prod_{l=2}^{k} \text{sign}\left(-\lambda_{i,l}\right) \times \min_{l=\{1,2\ldots,k\}}\left|\lambda_{i,l}\right|\right\} \quad (2\text{-}67)$$

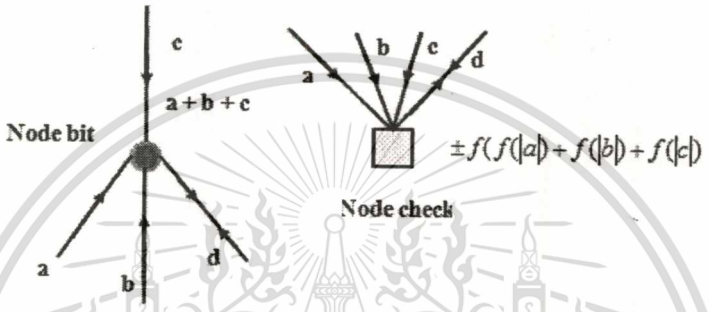

Figure 2.22 The function of bit node and checked node.

2.7 Thermal Asperity (TA)

To achieve ultrahigh storage capacity, magnetic recording systems use the magneto-resistive (MR) read head instead of the inductive heads. Practically, the MR read head directly senses flux via the transitions of the magnetic pattern written on the disk surface, resulting in an induced voltage pulse called a transition pulse. When an asperity (or a surface roughness) comes into contact with the slider, both the surface of the slider and the tip of the asperity are heated, which results in an additive voltage transient known as thermal asperity (TA) [2] in the readback signal. In general, the TA is considered as a defect. If the read head hits a dust particle, a long TA will occur, producing a severe transient noise burst, loss of timing synchronization, or even off-track perturbation. Typically, a TA signal has a short rise time ($60-150ns$) with a long decay time ($1-5\mu s$), and its peak TA amplitude could be 2 to 3 times the peak of the readback signal [2].

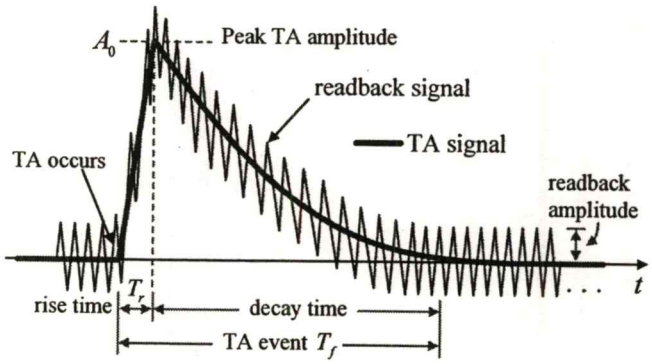

Figure 2.23 A widely used TA model associated with the MR read head [2].

TA signal model consists of following parameters.

START-TIME is the parameters which indicate where the TA impact comes from.

RISE-TIME is the rise time which is the linear parameter that controls the period to make the TA signal raised from base line to maximum amplitude of TA signal.

DECAY-CONSTANT is the go-down period in Exponential type and this parameter could reduce the TA signal to be only 1% of all TA signal.

MAX-AMPLITUDE is the maximum amplitude of TA signal since the TA signal is generated until the end of increasing time.

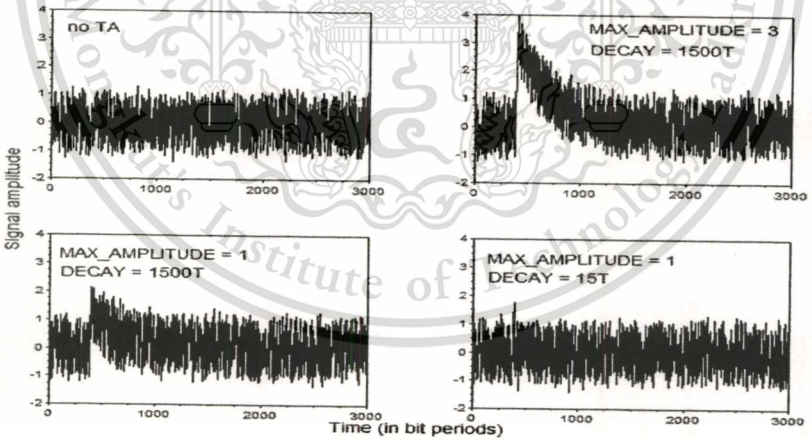

Figure 2.24 Types of impacts from TA in read back signal.

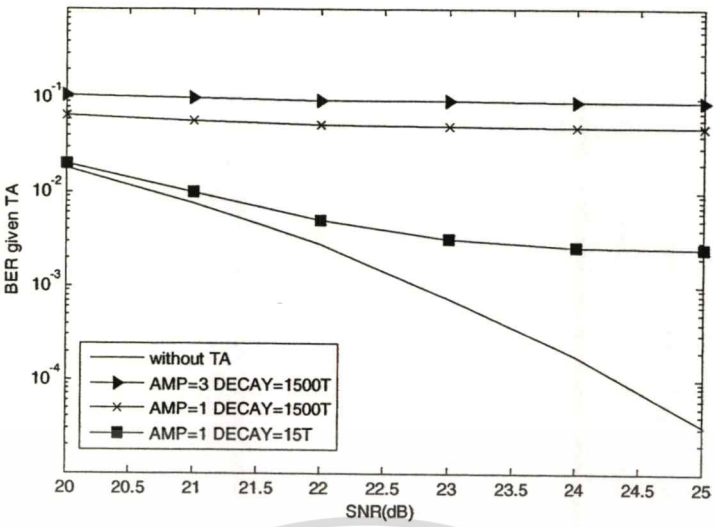

Figure 2.25 Types of impacted performances from TA.

Fig. 2.24 shows the types of impacts from TA in the readback signal and Fig. 2.25 shows the type of impacted performances from TA by used the perpendicular recording system when ND = 2 and EPR2 target is used. All those could be explained in $H(D) = 1+3D+3D^2+D^3$ and used 9-tap equalizer which has conditionally designed only target in section 2.3 when each sector had 4096 bit. The worst case scenario would be the one that is impacted by TA on any sector. In any serious impact from TA, they could not be fixed by [3], [5] error correction code and there could be a lot of errors in one sector if there is no reduction of impact from TA.

2.8 Literature Review

There are many reports about detection and correction of TA effect. These important studies are as follows;

Klaassen and Peppen [18] presented TA detection technique by comparison between read-back signal and average value of read-back signal. If there is no effect from TA, the average value of read-back signal or baseline value is usually equal to zero. The TA effect deduction is come from high pass filter of read-back signal.

Mathew and Tjhia [3] presented the detection method and the correction of TA effect. They showed that the baseline of read-back signal without effect from TA is equal to zero. However, the baseline value would not be equal to zero if there was some interfering from TA. They also demonstrated the method of re-calculation of the baseline from average value of read-back signal, the detection of TA from average value of read-back signal and threshold based approach and the correction by subtraction of average value of read-back signal from the read-back signal.

Dorfman and Wolf [17] demonstrated the algorithm of TA effect deduction

by using 1-*D* filtration system. ***D*** is a unit delayed operator. In the longitudinal recording channel, the effectiveness of the system was significant improved if using EPR4 as a target. However, there still were some problems about the correlated interfering signal. The improvement of effectiveness was done by using the noise predictive filter. [19] Nevertheless, 1-D was not appropriated to use in perpendicular recording channel because it composed of plenty of low frequency or D.C. component.

Erden and Kurta [4] showed the technique of detection and correction of TA in perpendicular recording channel. They used low and high pass filter to detect and estimate TA signal value by reducing TA effect prior to entering into the sampling system.

Kovintavewat and Koonkarnkhai [20, 21] presented TA effect deduction by estimating TA signal from the average value of read-back signal. They used linear correlation during the period of rise time and exponential correlation for the period of decay time before subtracting this value from read-back signal. Moreover, they also studied the impact of bandpass filter on TA effect deduction in the perpendicular recording channel. [22]

Chapter 3
Proposed Method

The objective of this chapter is to explain the effect of the thermal asperity (TA) suppression which is significant to the hard disk drive signal processing system. The technique and algorithm explained on this study is the joint iterative between thermal asperity suppression and turbo equalization in the perpendicular magnetic recording channel.

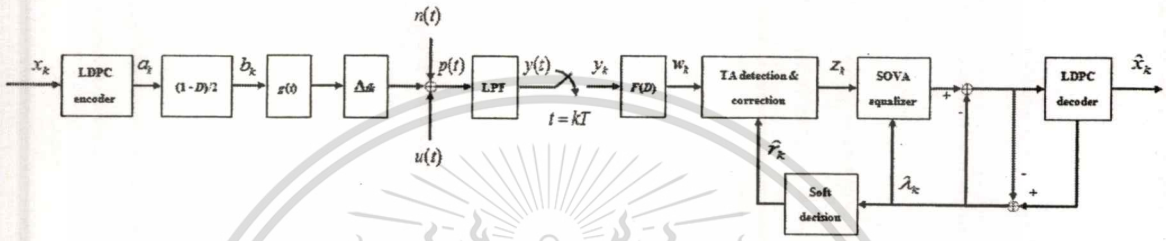

Figure 3.1 A perpendicular recording channel model with a TA suppression method.

3.1 Turbo equalization in perpendicular magnetic recording channels

This topic emphasizes the perpendicular recording channel and turbo equalization because it is now a common use for hard drive recording system. Fig. 3.1 shows the perpendicular recording channel model. The input sequence $x_k \in \{0, 1\}$ with bit period T will be encoded by an LDPC encoder [13], which gives a sequence $a_k \in \{\pm 1\}$. Then, the sequence a_k passes through an ideal differentiator filter $(1-D)/2$, where D is a unit delay operator, to obtain a transition sequence $b_k \in \{0, \pm 1\}$, where ± 1 is positive and negative transition and 0 is no transition. The read-back signal is shown as

$$p(t) = \sum_k b_k g(t - kT - \Delta t_k) + n(t) + u(t) \qquad (3\text{-}1)$$

where g(t) = $\text{erf}(t\sqrt{\ln 16} / \text{PW}_{50})$ is transition response in perpendicular recording channel [23], PW50 is pulse width at the half of its maximum, erf(x) is error function, n(t) is additive white Gaussian noise (AWGN) with two-sided power spectrum density N0/2, u(t) is TA signal, and Δtk is media jitter noise [23], that occurred by the shift of randomized status change which has the Gaussian probability density function which

arithmetic mean is equal to zero and variance is equal to $|b_k|\sigma_j^2$ but not more than T/2, σ_j is the percentage of bit cell T.

In general, TA signal model in Fig. 2.23 represented by Stupp et al. [2] is commonly used. This TA model is comparable to the data from the HDD recorder, which shows linear correlation during the rise time period and exponential correlation in the decay time period, according to the following equation [3]

$$u(t) = \begin{cases} A_0 t / T_r, & 0 \le t \le T_r \\ A_0 \exp(-(t - T_r)/T_d), & T_r < t \le T_f \end{cases} \quad (3\text{-}2)$$

where A_0 is maximum amplitude of TA signal, T_r is rise time period, T_d is decay constant in the decay time period, and total time of TA signal is $T_f = T_r + 4T_d$, which $4T_d$ is sufficient to reduce the maximum amplitude of TA to 1.8%.

In the common receiving circuit, when the TA effect is reduced, the output will be sent to the soft-output Viterbi algorithm (SOVA) circuit [11] and the LDPC decoding circuit [13], which iteratively exchanges soft information between SOVA and LDPC circuits, according to a given number of iterations. Clearly, this scheme does not exploit the soft data from the LDPC decoding circuit to reduce the TA effect.

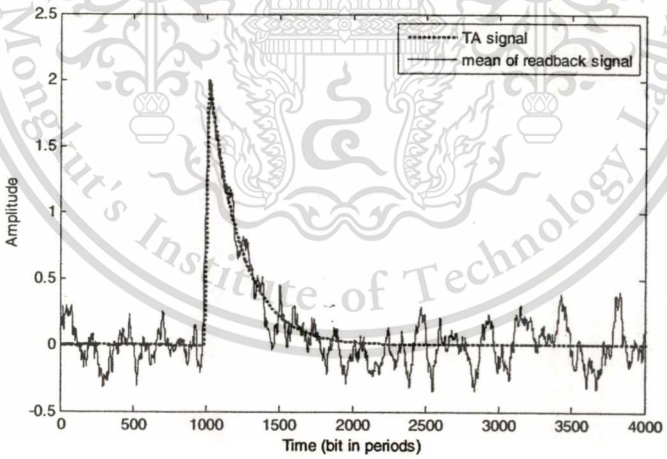

Figure 3.2 TA signal and an averaged read-back signal $\{q_k\}$.

3.2 TA effect suppression technique

This topic will explain the technique of conventional TA suppression [20], which has been modified to use in turbo equalization channel. Then, we discuss about the iterative TA detection and correction algorithm designed for a perpendicular recording channel, which has been presented by Thongkam *et al.* [24]

3.2.1 Conventional TA effect suppression technique

As in the Fig. 3.1, the data sequence $\{w_k\}$ at the output equalizer $F(D)$ will be sent to the TA detection and correction circuit. The TA detection starts from finding out the baseline of the read-back signal according to [3]

$$q_k = \frac{1}{L}\sum_{i=k-\alpha}^{k+\alpha} w_i \tag{3-3}$$

where w_i is the i-th sample of the equalizer output $\{w_k\}$, L is the width of the window that is used for calculating the average value, and $\alpha = (L-1)/2$. The TA will be detected when $q_k \geq n$ when $n > 0$ is a threshold value.

Fig. 3.2 shows the mean of read-back signal q_k is similar to signal TA. Therefore curve fitting technique is used to reconstruct the TA signal. The TA signal period is separated into 2 parts, rise time part and decay part. The linear fitting technique is applied for the rise time part. For the decay part, 2 curve fitting techniques, polynomial fitting and exponential fitting, are compared in order to select the best. The polynomial fitting technique provides the better result in term of bit error rate (BER) [20-21]. Therefore, exponential fitting technique is selected for decay part in this research.

The estimation of rise time part starts from the detection of TA effect. The values of $\{q_k\}$ are collected and averaged for estimating the rise time part of TA signal. The values of $\{q_k\}$ are sampled at the time the TA signal detected to the maximum value of $\{q_k\}$. Then linear fitting as stated in the previous paragraph is applied. The equation of linear fitting is as below

$$\hat{u}_r(t) = at + b \tag{3-4}$$

where $\hat{u}_r(t)$ is estimate value of TA signal in the rise time period a, b are coefficient of the linear equation which come from the solution of the equation (3-5)

$$\begin{bmatrix} \sum_{i=1}^{m} t_i^2 & \sum_{i=1}^{m} t_i \\ \sum_{i=1}^{m} t_i & m \end{bmatrix} \begin{bmatrix} a \\ b \end{bmatrix} = \begin{bmatrix} \sum_{i=1}^{m} t_i q_i \\ \sum_{i=1}^{m} q_i \end{bmatrix} \quad (3\text{-}5)$$

where q_i is i-th sample of the average read-back signal, and m is number of total sample which is used for the signal estimation.

The decay time part is estimated by, starting from the maximum value of $\{q_k\}$ and continue collecting the data to $4T_d$ period, where T_d is period of rise-time part. The decay time part is estimated by exponential fitting equation as below

$$\hat{u}_{d,\exp}(t) = Ae^{Bt} \quad (3\text{-}8)$$

where $\hat{u}_{d,\exp}(t)$ is estimate value of TA signal in the decay time period, exponential pattern A and B is coefficients of exponential equation when $A = \exp(z)$ the equation is shown below [20].

$$z = \frac{\sum_{i=1}^{n}\left(t_i^2 q_i\right)\sum_{i=1}^{n}\left(q_i \ln q_i\right) - \sum_{i=1}^{n}\left(t_i q_i\right)\sum_{i=1}^{n}\left(t_i q_i \ln q_i\right)}{\sum_{i=1}^{n}\left(q_i\right)\sum_{i=1}^{n}\left(t_i^2 q_i\right) - \left(\sum_{i=1}^{n} t_i^2 q_i\right)^2} \quad (3\text{-}9)$$

$$B = \frac{\sum_{i=1}^{n}\left(q_i\right)\sum_{i=1}^{n}\left(t_i q_i \ln q_i\right) - \sum_{i=1}^{n}\left(t_i q_i\right)\sum_{i=1}^{n}\left(q_i \ln q_i\right)}{\sum_{i=1}^{n}\left(q_i\right)\sum_{i=1}^{n}\left(t_i^2 q_i\right) - \left(\sum_{i=1}^{n} t_i^2 q_i\right)^2} \quad (3\text{-}10)$$

where q_i is i–th sample of the average read-back signal, n is number of total sample which is used for the signal estimation. The estimation process of decay time part is complete when $\hat{u}_{d,\exp}(t) < 0.01$. The estimation processes (rise time estimation and decay time estimation) then are combined to be the complete estimation of TA signal as below

$$\hat{u}(t)=\begin{cases}\hat{u}_r(t), & T_y \le t \le \hat{T}_r \\ \hat{u}_d(t), & \hat{T}_r < t \le \hat{T}_f\end{cases} \quad (3\text{-}11)$$

where T_y is point when detects TA effect, $\hat{T}_r$ is time when sample q_k reaches the maximum value, $\hat{T}_f$ is time period of signal $\hat{u}(t)$ starting from T_y until reaching the time of the signal < 0.01.

The estimated TA signal then is subtracted from the data sequence a the output limb of equalizer circuit $\{w_k\}$, as shown below

$$z_k=\begin{cases}w_k - \hat{u}_k, & \text{if TA is present} \\ w_k, & \text{if TA is absent}\end{cases} \quad (3\text{-}12)$$

where z_k is signal output from TA effect suppression, w_k is sequence of data at the output limb of equalizer circuit, $\hat{u}_k$ is estimate TA signal value when $\hat{u}(t)=\hat{u}(kT)=\hat{u}_k$. When the data sequence passes TA effect suppression is feed to Veterbi detection circuit. This process is terminated as the conventional TA effect suppression is considered.

3.2.2 Co-operation between TA effect suppression and turbo equalization

In this study, the soft decision block is proposed into the conventional block diagram. The soft decision block feeds the signal from LDPC decoder back to the TA detection and correction block (refer to Fig. 3.1). This approach is expected to use soft information from LDPC decoder to get better on TA detection and correction. The algorithm of soft decision block is explained in chapter 4.

Chapter 4
Simulation Results

The simulation result was organized as follows. After explaining a system model in the first section, then the next section briefly describes how the iterative TA suppression method works and then summarizes the iterative TA suppression method and complexity. Eventually, numerical results are provided in the last section.

4.1 Channel model

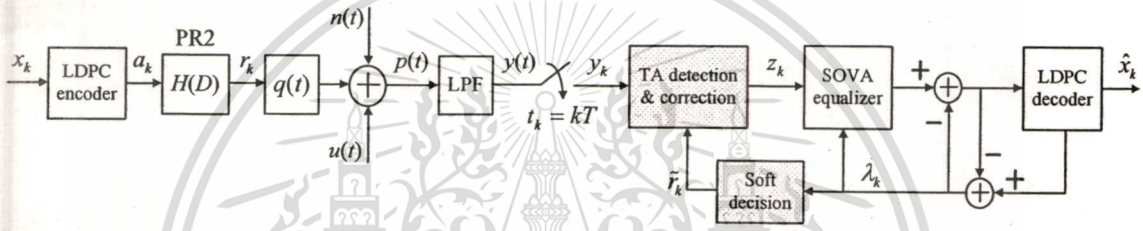

Figure 4.1 A channel model with an iterative TA suppression method.

Consider a rate-8/9 coded partial-response (PR) channel illustrated in Fig. 4.1, where a block of 3640 message bits $x_k \in \{0, 1\}$ is encoded by a regular $(j, k) = (3, 27)$ low-density parity-check (LDPC) code [10], resulting in a coded block length of 4095 bits $a_k \in \{\pm 1\}$ with bit period T. The parity-check matrix has 3 ones in each column and 27 ones in each row. The readback signal can then be expressed as

$$p(t) = \sum_k r_k q(t - kT) + n(t) + u(t) \qquad (4\text{-}1)$$

where $r_k = a_k * h_k \in \{0, \pm 2, \pm 4\}$ is the noiseless channel output, $*$ is the convolution operator, $q(t) = \sin(\pi t/T)/(\pi t/T)$ is an ideal zero-excess-bandwidth Nyquist pulse, $n(t)$ an additive white Gaussian noise (AWGN) with two-sided power spectral density $N_0/2$, and $u(t)$ is a TA signal.

A widely used TA model described by Stupp *et al.* [2] is considered as shown in Fig. 2.23, because it fits captured spin stand data and drive data very well [4]. This TA signal has a short rise time with a long decay time, and its effect is assumed to decay exponentially, which can be modeled as

$$u(t)=\begin{cases}A_0 t/T_r, & 0\le t\le T_r\\ A_0\exp\left(-(t-T_r)/T_d\right), & T_r<t\le T_f\end{cases} \quad (4\text{-}2)$$

where $A_0=\beta\sum_k|h_k|$ is the peak TA amplitude, $\beta\ge 0$ is the peak-factor, T_r is a rise time, and T_d is a decay constant. In this paper, the TA duration is assumed to be $T_f = T_r + 4T_d$ [3], where a decay time of $4T_d$ is sufficient because it will reduce the amplitude of the TA signal to approximately 1.8% of its peak amplitude. At the receiver, the readback signal $p(t)$ is filtered by an ideal low-pass filter (LPF), whose impulse response is $q(t)/T$, to eliminate out-of-band noise, and is then sampled at a symbol rate of 500 Mbps [3], assuming perfect synchronization. The sampler output, y_k, is fed to the TA detection/correction block to obtain the corrected readback signal, z_k.

In a conventional setting, the TA detection/correction block is followed by a turbo equalizer, which iteratively exchanges soft information between the soft-output Viterbi algorithm (SOVA) [11] equalizer for the PR2 channel and the LDPC decoder (implemented based on the message-passing algorithm [11] with N_{in} = 3 internal iterations) for the outer code.

4.2 Existing TA suppression method

This simulation focuses only on two TA suppression methods (i.e., one is based on a threshold-based technique, and the other is based on an LS fitting technique) because of its simplicity. We briefly explain how the two methods operate as follows.

4.2.1 Threshold-Based Technique

We denote the TA suppression method based on a threshold-based technique [3] as "**M1**," where the TA detection method is performed by first finding the average value of the readback signal, q_k, according to

$$q_k=\frac{1}{L}\sum_{i=k-\alpha}^{k+\alpha} y_i \quad (4\text{-}3)$$

where y_i is the i-th sample of the readback signal, α is an integer, and $L = 2\alpha + 1$ is the window length for computing q_k. Then, a TA is detected if $q_k \ge n_1$ and $y_i \ge n_2$ for a few consecutive samples, where n_1 *and* n_2 are threshold values.

After the TA is detected, the TA detection operation is disabled and the TA correction operation is activated for duration of T_f. Then, the TA-unaffected readback signal, z_k, is obtained by subtracting the reconstructed TA signal from the TA-affected readback signal according to

$$z_k = \begin{cases} y_k - q_k, & \text{if TA is present} \\ y_k, & \text{if TA is absent} \end{cases} . \quad (4\text{-}4)$$

4.2.2 Least-Squares Fitting Technique

Again, we denote the TA suppression method based on the LS fitting technique [20] as "M2." To detect a TA, we first find the averaged readback signal, q_k, from equation (4-3). Then, the TA is detected if only $q_k \geq n_1$.

After the TA is detected, the TA detection operation is disabled and the TA correction operation is activated for a duration of T_f so as to construct the estimated TA signal, $\hat{u}(t)$, based on the LS fitting technique and the samples $\{q_k\}$ [20]. This can be achieved by estimating the TA signal during a rise time and a decay time, where the TA signal during a rise time is approximately linear, whereas that during a decay time is exponentially decay [2]. Hence, the corrected readback signal is obtained from equation (4-4) by replacing q_k by $\hat{u}_k$, where $\hat{u}_k = \hat{u}(kT)$ is the k-th estimated TA sample.

4.3 Iterative TA Suppression Method

A conventional receiver sends a sequence $\{z_k\}$ directly to the turbo equalizer. Specifically, the TA suppression method ignores the presence of ECCs, and is thus doomed to fail when the SNR is low enough. To solve this problem, the iterative TA suppression method was proposed in [5], where the TA detection/correction block, the SOVA equalizer, and the LDPC decoder exchange information as shown in Fig. 4.1. This thesis investigates the performance of the two iterative TA suppression methods, one is based on M1 and the other is based on M2.

Denote the first time that the SISO decoder outputs the soft information λ_k as the first iteration. Clearly, the iterative scheme performs the same operations as the conventional receiver does at the first iteration. Nevertheless, after the first iteration, the soft information λ_k is fed back to both the SOVA equalizer and the TA detection/correction block. Then, an improved set of samples $\{z_k\}$ can be obtained by running the TA suppression method again, but this time it is performed on a sequence $\{c_k\}$, where $c_k = y_k - \tilde{r}_k$, $\tilde{r}_k = E[r_k \mid \lambda_k]$ is the k-th soft decision of r_k, and $E[\cdot]$

is the expectation operator. It can be shown that for a PR2 channel, the soft decision is given by [5]

$$\tilde{r}_k = \frac{A+B+C}{2\cosh(\lambda_k/2)\cosh(\lambda_{k-1}/2)\cosh(\lambda_{k-2}/2)} \tag{4-5}$$

where $A = 2\sinh((\lambda_k + \lambda_{k-1} + \lambda_{k-2})/2)$, $B = \sinh((\lambda_k + \lambda_{k-1} - \lambda_{k-2})/2)$, $C = \sinh((-\lambda_k + \lambda_{k-1} + \lambda_{k-2})/2)$

Consequently, the improved samples $\{z_k\}$ are fed to the turbo equalizer, which generally yields an improved set of soft decisions $\{\tilde{r}_k\}$. The process repeats as many turbo iterations as required. It is evident that the turbo equalizer benefits from better samples $\{z_k\}$, and the TA suppression method benefits from better decisions $\{\tilde{r}_k\}$.

4.4 Complexity Comparison

To measure the complexity of iterative schemes, we consider the total number of additions and multiplications (per bit) as a criterion. Table (4-1) shows the complexity of each component, where $Q = 2^{\nu}$ is the number of trellis states [26]; ν is the target memory; δ is the decoding depth used in SOVA [11]; k is a parameter of an LDPC code [13]; N_{in} is the internal iterations used in the LDPC decoder; R is a code rate; P is the number of bits per sector, C is an indicator such that $C = 0$ if $N = 1$, and $C = 1$ if $N > 1$, and N is the number of turbo iteration. For a coded PR2 channel, the complexity of each iterative TA suppression methods is given in Table 2, where $\nu = 2$, $Q = 4$, $L = 51$, $\delta = 15$, $N_{in} = 3$, $k = 9$, $T_d = 1000T$, $T_r = 30T$, $T_f = 1030T$, $R = 8/9$, and $P = 4095$ bits.

Table 4-1 The total number of operations (per bit) of each function.

Module	Number of operations (per bit)	
	Addition	Multiplication
SOVA	$7Q + \frac{\delta^2+9\delta+9}{2} + 1$	$6Q + 1$
LDPC decoder	$(1 + (k - 1)(1 - R))N_{in} + 1$	$(1 - R)N_{in}$
Data exchange	2	0
Soft decision	8	9
M1	$(L - 1) + T_f/P + C$	1
M2	$\{(L - 1)P + 14T_d + 5T_r + T_f - 11\}/P + C$	$\{P + 18T_d + 2T_r + 11\}/P$

Table 4-2 Complexity (per bit) of different iterative TA suppression methods.

System	Number of operations (per bit)	
	Addition	Multiplication
Conventional receiver with M1	$50.251 + 222.17N$	$1 + 25.333N$
Iterative TA with M1	$(280.42 + C)N$	$35.333N$
Iterative TA with M2	$(283.87 + C)N$	$39.744N$

It is of interest to compare the performance of different TA suppression methods when they have same complexity. Since multiplication has much more complexity than addition in terms of circuit implementation, we consider only the number of multiplications when comparing performances. Suppose that current technology can support the total number of multiplications equal to 10 iterations of the iterative TA suppression method with M2. It is clear from Table 2 that 10 iterations of the iterative TA suppression method with M2 are approximately equal to 11 iterations of that with M1, and 14 iterations of the conventional receiver (which utilizes the M1 to mitigate the TA effect at the first iteration only).

4.5 Numerical Result

In simulation, every 4095-bit data sector is corrupted by one TA at the 500-th bit with β = 2, T_r = 60 ns, and T_d = 0.5 μs (i.e., a TA event T_f = 1030T) [3]. We compute the BER based on a minimum number of 10000 data sectors and 1000 error bits, and call that number as "BER given TA." For the PR2 channel, L = 51, n_1 = 2.8, and n_2 = 4.5 are suitable parameters for TA detection [5, 20].

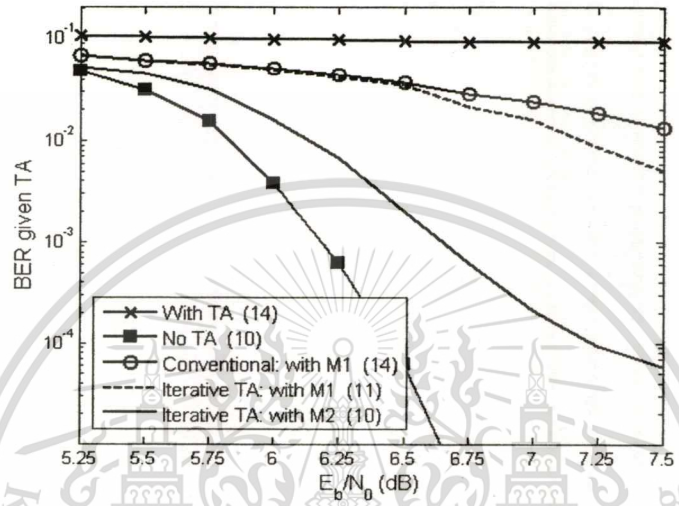

Figure 4.2 Performance comparisons of different schemes with same complexity.

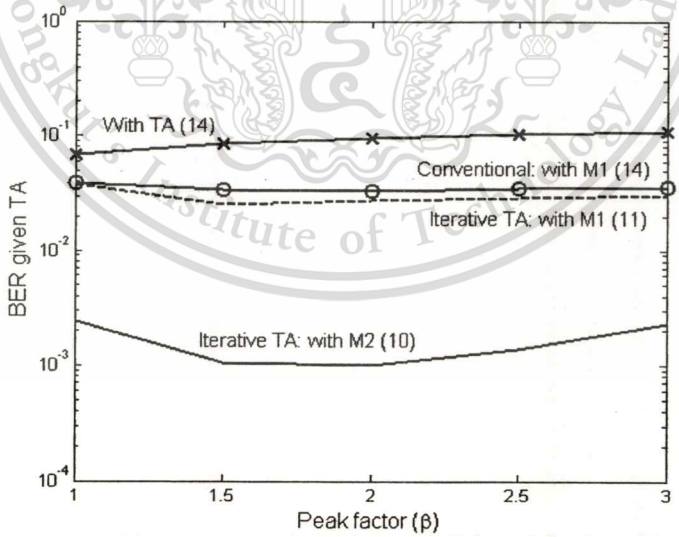

Figure 4.3 BER performances with different peak factors.

Fig. 4.2 compares the performance of different schemes when they have same complexity, where the number inside the parenthesis indicates the number of iterations used to generate each curve, and the system performance in the absence of TA is referred to as "No TA." It is obvious that without the TA suppression method, the system performance is unacceptable, denoted as "With TA." As depicted in Fig. 4.2, the iterative TA suppression method with M2 outperforms that with M1 and the conventional receiver.

We also compare the performance of different schemes as a function of peak factors in Fig 4.3. As expected, with same complexity, the iterative TA suppression method with M2 still outperforms that with M1 and the conventional receiver for all peak factors. This might be because the TA suppression method based on the LS fitting technique (i.e., M2) performs better than that based on the threshold-based technique (i.e., M1) as studied in [20].

4.6 Comparison of performance in realistic magnetic recording channel model with media jitter noise effect

Fig 3.1 shows iterative realistic magnetic recording channel model with media jitter noise effect. Consider a perpendicular recording channel at ND = 2 or Du = 2.25 (user density), when 8/9-rate LDPC code is used with 3% media jitter noise ($\sigma j/T$ = 3%). The 11- tap equalizer and 4-tap target ware designed based on the minimum mean-squared error (MMSE) approach at SNR required to achieve BER $=10^{-4}$ without the LDPC and the media jitter noise and the TA is absent. The 4-tap GPR target is given by $H(D) = 1+1.1295D+0.51092D^2$.

In the simulation, every 4095-bit data sector is corrupted by one TA at the 500-th bit with with A0 = 2, Tr = 60 ns, and Td = 0.5μs (i.e., a TA event Tf = 1030T). We compute the BER based on the minimum number of 10000 data sectors and 1000 error bits, and call that number "BER given TA." For the PR2 channel, L = 51, n = 2.8 are the suitable parameters for TA detection.

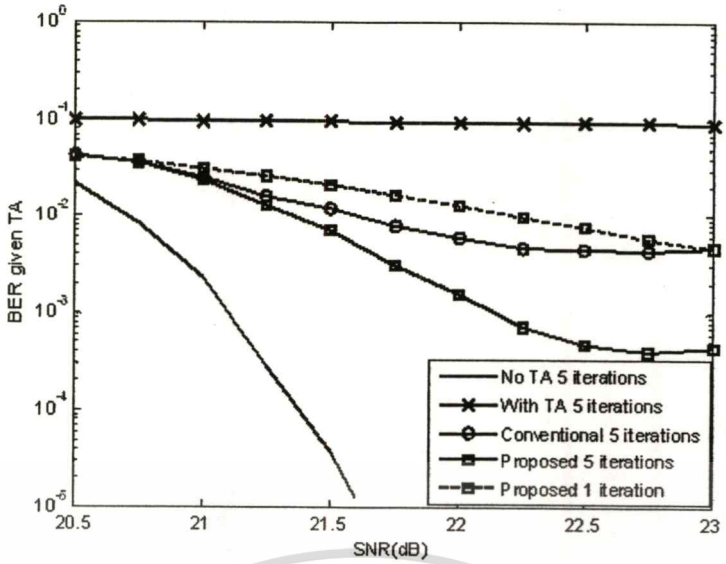

Figure 4.4 Performance comparisons of different schemes at 5-th iteration in terms of SNR.

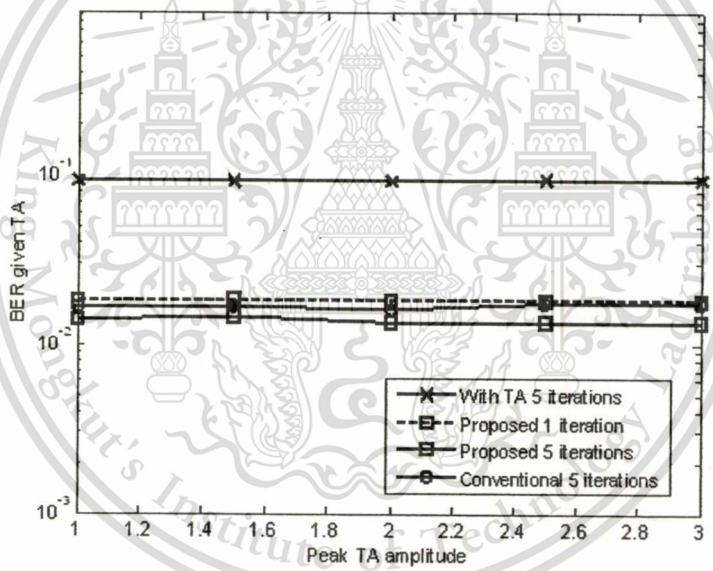

Figure 4.5 Performance comparisons of different schemes at 5-th iteration in terms of TA amplitude.

Figs. 4.4 and 4.5 compare the performance of different schemes in terms of SNR and TA amplitude, where the number indicates the number of iterations used to generate each curve, and the system performance in the absence of TA is referred to as "No TA." It is obvious that without the TA suppression method, the system performance is unacceptable, denoted as "With TA." The system performance with non-iterative TA is referred to as "Conventional" and with iterative TA method is referred as "Proposed." As depicted in Fig. 4.4 and Fig. 4.5 the iterative TA suppression method performs better than the non-iterative method.

Chapter 5
Conclusions and Suggestions

5.1 Conclusions

The TA highly affects the performance of perpendicular magnetic recording systems. From the simulation results, the performance is not acceptable if there is no TA suppression technique even if there is the iterative decoding circuit in the system. This study presents the cooperation between the TA suppression algorithm and the turbo equalization by using the soft information from the LDPC decoding circuit to suppress the TA effect in each round of decoding process. The results show that the proposed technique performs better than the conventional technique and is more robust to the change of TA maximum amplitude. Also, at the same level of complexity (addition and multiplication operation), the proposed algorithm still performs better than the conventional one.

5.2 Problem in this research

Consider the low SNR scenario, the effect of noise will impact the quality of soft information (λ_k) from LDPC. Therefore, the improvement set of soft decisions ($\tilde{r}_k$) from soft decision block will also be negatively impact which also impacted the TA detection and correction. Further study of low SNR scenario should be valuable for improving the output of soft decision block.

5.3 Suggestions

In perpendicular magnetic recording systems, the TA problem results from not only the MR read head but recently also the tunneling magneto resistive (TuMR) read head, where the TA resulted from the TuMR read head will look different. Thus, there should be some adjustment on the iterative TA detection and correction algorithm when using in HDDs with the TuMR read head because of a new TA signal.

Reference

[1] P. Kovintavewat. "Signal processing for data storage Vol.1: Basic read-write channel," **National Electronic and Computer Technology Center (NECTEC)**, 2007.

[2] S. E. Stupp, et al. "Thermal asperity trends," **IEEE Transactions Magnetics**, vol. 35, no. 2, pp. 752-757, 1999.

[3] G. Mathew and I. Tjhia. "Thermal asperity suppression in perpendicular recording channels," **IEEE Transactions Magnetics**, vol. 41, no. 10, pp. 2878-2880, 2005.

[4] M. F. Erden, and E. M. Kurtas. "Thermal asperity detection and cancellation in perpendicular recording systems," **IEEE Transaction on Magnetics**, vol.40, no. 3, pp. 1732–1737, 2004.

[5] P. Kovintavewat and S. Koonkarnkhai. "Joint TA suppression and turbo equalization for magnetic recording channel," **IEEE Transaction on Magnetics**, vol. 46, no.6, pp. 1393 – 1396, 2010.

[6] B. Vasic, and E. M. Kurtas. "Coding and signal processing for magnetic recording systems," **CRC Press**, 2005

[7] Y. Shiroishi, K. Fukuda, et al. "Future options for HDD storage," **IEEE Transactions on Magnetics**, Vol. 45, No. 10, pp. 3816-3822, 2009.

[8] T. A. Roscamp, E. D. Boerner, and G. J. Parker. "Three-dimensional modeling of perpendicular recording with soft underlayer," **Journal of Applied Physics**. vol. 91, no. 10, 2002.

[9] M. F. Erden, and et al. "General transform filter in perpendicular recording architectures," **IEEE Transactions on Magnetics**, vol. 38, no. 5, pp. 2334 – 2336, 2002.

[10] P. Kovintavewat. "Signal processing for digital data storage vol.3 Advanced receiver design," **Phetkasem Printing Group Co., Ltd.** 2011.

[11] J. Hagenauer and P. Hoeher "A Viterbi algorithm with soft-decision outputs and its applications," **in Proc. of Globecom'89**, pp. 1680 – 1686, 1989.

[12] T. Souvignier, A. Friedmann, M. Oberg, P. Siegel, R. Swanson, and J. Wolf. "Turbo decoding for PR4: parallel vs. serial concatenation," **in Proc. of ICC'99**, vol. 3, pp. 1638-1642, 1999.

[13] R. Gallager. "Low-density parity-check codes," **IRE Trans. on Inform. Theory**, vol. IT-8, pp. 21-28, 1962.

[14] P. Kovintavewat. "Signal processing for data storage Vol. 2: Receiver design," **National Electronic and Computer Technology Center (NECTEC)**, 2007.

[15] J. Moon, and W. Zeng. "Equalization for maximum likelihood detector," **IEEE Transaction on Magnetics.** vol. 31, pp. 1083 – 1088, 1995.

[16] L. R. Bahl, J. Cocke, F. Jelinek, and J. Raviv. "Optimal decoding of linear codes for minimizing symbol error rate," **IEEE Transactions on Information Theory,** IT-20, pp. 248 – 287, 1974.

[17] V. Dorfman and J. K.Wolf. "A method for reducing the effects of thermal asperities," **IEEE Journal Selected Areas Communications,** vol. 19, no. 4, pp. 662–667, 2001.

[18] K. B. Klaassen and J. C. L. van Peppen. "Electronic abatement of thermal interference in (G)MR head output signals," **IEEE Transaction on Magnetics,** vol. 40, pp. 2611-2616, 1997.

[19] V. Dorfman and J. K. Wolf. "Viterbi detection for partial response channels with colored noise," **IEEE Transaction on Magnetics**, vol. 38, pp. 2316–2318, 2002.

[20] P. Kovintavewat, and S. Koonkarnkhai. "Thermal asperity suppression based on least squares fitting in perpendicular magnetic recording systems," **Journal of Applied Physics**, vol. 105, no. 7, 2009.

[21] S. Koonkarnkhai. "Development of thermal asperity detection and correction algorithm for magnetic recording channels (in Thai)," **Master thesis, King Mongkut's University of Technology North Bangkok,** 2009.

[22] S. Koonkarnkhai, P. Kovintavewat, and P. Keeratiwintakorn. "Effect of Bandpass Filters for TA Suppression in Perpendicular Recording System," **Transactions on ECTI-EEC**, vol. 8, no. 1, pp. 93 – 98, 2010.

[23] P. Kovintavewat, I. Ozgunes, E. M. Kurtas, J. R. Barry, and S. W. Mclaughin. "Generalized partial response target for perpendicular recording with jitter noise," **IEEE Transaction on Magnetics**, vol. 38, no. 5, pp. 2340-2342, 2002.

[24] T. Thongkam, S. Koonkarnkhai, P. Kovintavewat, P. Supnithi. "Performance of Iterative Joint Thermal Asperity Suppression and Turbo Equalization in Perpendicular Magnetic Recording Channel (in Thai)," **Proceeding Electrical Engineering Conference**, 2010.

[25] T. Thongkam, S. Koonkarnkhai, P. Kovintavewat, P. Supnithi. "Investigation of Iterative TA Suppression Method in Perpendicular Recording System," **Proceeding Data Storage Technology Conference**, 2010.

[26] G. D. Forney. "Maximum-likelihood sequence estimation of digital sequences in the presence of inter symbol interference," **IEEE Trans. Inform. Theory**, vol. IT-18, no. 3, pp. 363 – 378, 1972.

[27] R.M. Tanner. "A recursive approach to low complexity codes," **IEEE Trans. Inform. Theory**, vol. IT-27, pp. 533-547, 1981.

[28] F.R. Kschischang, B. J. Frey, and H.-A. Loeliger. "Factor Graphs and the Sum-Product Algorothm," **IEEE Trans. Inform. Theory**, vol. 47, no. 2, pp. 498-519, 2001.

Appendix

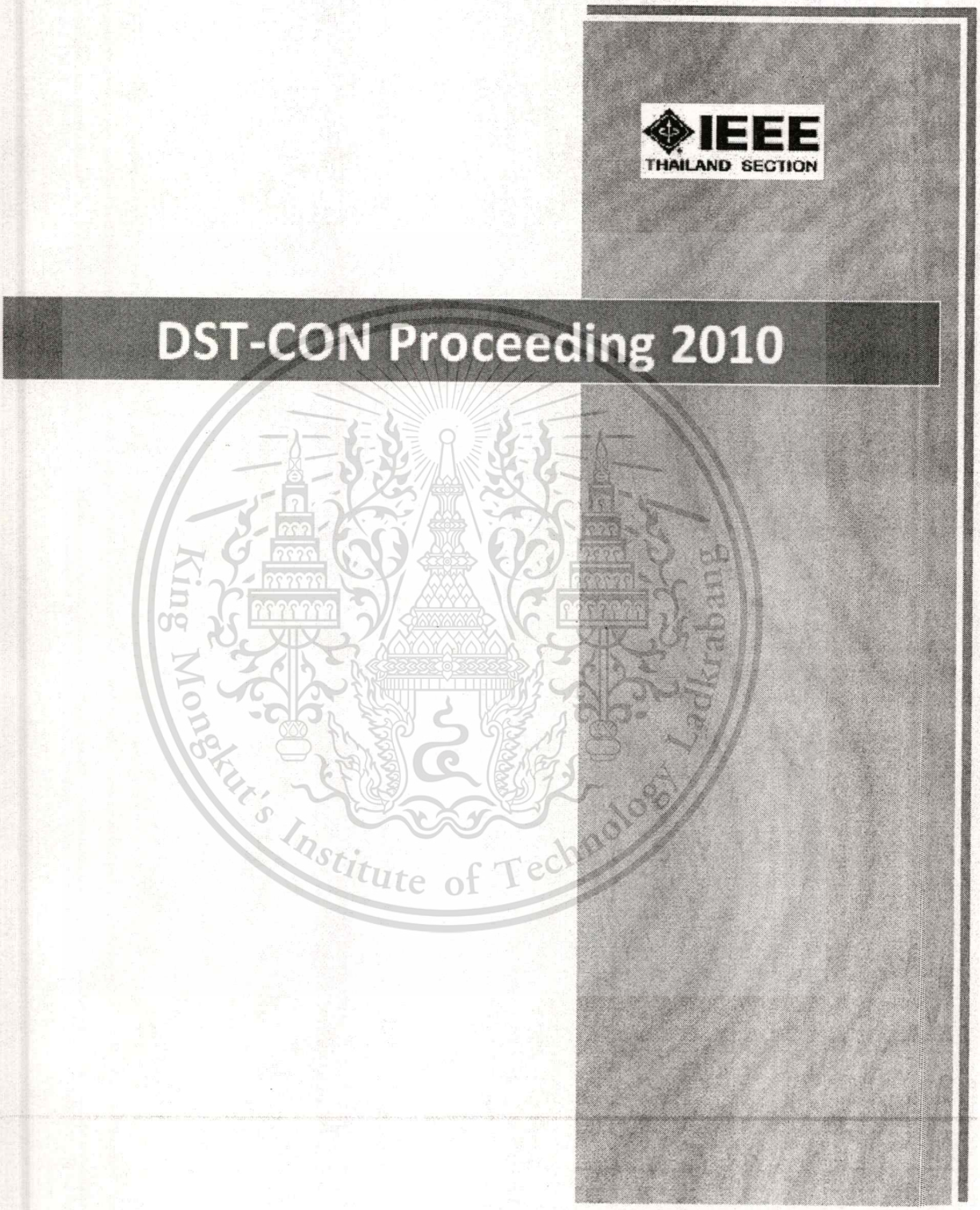

Investigation of Iterative TA Suppression Method in Perpendicular Recording System

T. Thongkam*, S. Koonkarnkhai**, P. Kovintavewat***, P. Supnithi****
*) T. Thongkam is with College of Data Storage Technology and Applications, I/U CRC in Data Storage Technology and Applications (D*STAR), Bangkok 10520, KMITL, Thailand. ;e-mail: theerachat.thongkam@wdc.com).
**) S. Koonkarnkhai is with Department of Electrical Engineeiring, KMUTNB, Thailand. (e-mail: s5010182144@kmutnb.ac.th).
***) P. Kovintavewat is with Data Storage Technology Research Unit, Nakhon Pathom Rajabhat University, Nakhon Pathom 73000, Thailand. (e-mail: piya@npru.ac.th).
****) P. Supnithi is with Faculty of Engineering, KMITL, Bangkok 10520, Thailand. (e-mail: ksupornc@kmitl.ac.th).

Abstract— **Thermal asperities (TAs) cause a critical problem in perpendicular recording systems because they can distort the readback signal to the extent of causing an error burst in data detection process. System performance without a TA detection and correction algorithm can be unacceptable, depending on how severe the TA effect is. This paper investigates the performance of an iterative TA suppression method, which jointly performs TA suppression and turbo equalization on coded partial-response channels. Specifically, two iterative TA suppression methods are compared (i.e., one is based on a threshold-based technique, and the other is based on a least-squares (LS) fitting technique) in terms of bit-error rate performance and complexity. Results indicate that two methods have comparable complexity, but the method based on a LS fitting technique performs better than that based on a threshold-based technique. Thus, it is worth employing the iterative TA suppression method based on the LS fitting technique in perpendicular recording systems.**

Index Terms—Coded partial-response channel, iterative method, thermal asperity detection and correction, turbo equalization.

I. Introduction

To achieve ultra high storage capacity, magnetic recording systems use the magneto-resistive (MR) read head instead of the inductive heads. Practically, the MR read head directly senses flux via the transitions of the magnetic pattern written on the disk surface, resulting in an induced voltage pulse called a *transition pulse*. When an asperity (or a surface roughness) comes into contact with the slider, both the surface of the slider and the tip of the asperity are heated, which results in an additive voltage transient known as *thermal asperity* (TA) [1] in the readback signal.

In general, the TA is considered as a defect. If the read head hits a dust particle, a long TA will occur, producing a severe transient noise burst, loss of timing synchronization, or even off-track perturbation. Typically, a TA signal has a short rise time (50 – 160 ns) with a long decay time (1 – 5 μs), and its peak TA amplitude could be 2 to 3 times the peak of the readback signal [1].

Several TA detection and correction algorithms have been proposed in the literature [2] – [7] to alleviate the TA effect. The average value of the normal readback signal is zero, whereas that of the TA-affected readback signal is not because the TA causes a shift in the baseline of the readback signal. Thus, Klaassen and van Peppen [2] proposed the TA detection that looks at the baseline of the averaged readback signal, while the TA correction was done by use of a high-pass filter. Dorfman and Wolf [3] proposed a method to reduce the TA effect by passing the TA-affected readback signal through a filter $(1 - D)$, where D is a delay operator. This method is good for a longitudinal recording channel, but not for a perpendicular recording channel because this channel has a d.c. component. For perpendicular recording channels, Erden and Kurtas [4] proposed a TA suppression method by use of different low-pass and high-pass filters, while Mathew and Tjhia [5] proposed a simple threshold-based technique to detect and suppress the TA effect, Kovintavewat and Koonkarnkhai [6] proposed a TA suppression method based on a least-squares fitting technique, which performs better than the method proposed in [5] at the expense of increasing complexity.

All TA suppression methods mentioned above were proposed for the system without ECCs. Because of a large coding gain of ECCs, a reliable communication can be operated at very low signal-to-noise ratio (SNR) [8]. This means that the TA suppression method must be performed at an SNR lower than ever before. Therefore, a conventional receiver, which performs TA suppression and turbo equalization *separately*, is doomed to fail when the SNR is low enough. To solve this problem, Kovintavewat and Koonkarnkhai [7] proposed an iterative TA suppression method based on a least-squares fitting technique, to *jointly* performing TA suppression and

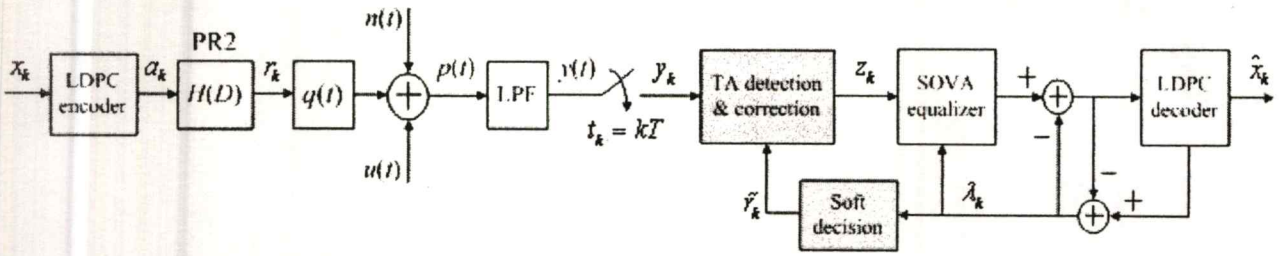

Fig. 1. A channel model with an iterative TA suppression method.

turbo equalization [9]. This paper investigates and compares the performance of the iterative TA suppression methods based on a least-squares fitting technique and a threshold-based technique in terms of bit-error rate (BER) and complexity.

The paper is organized as follows. After explaining a system model in Section II, Section III briefly describes how the iterative TA suppression method works. Section IV summarizes the iterative TA suppression method. Complexity issue is given in Section V. Numerical results are provided in Section VI. Eventually, Section VII concludes this paper.

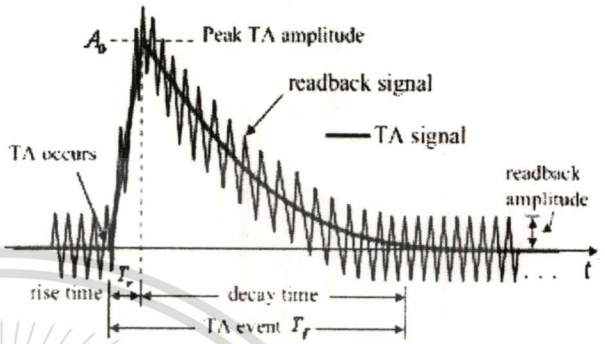

Fig. 2. A widely used TA model associated with the MR read head.

II. Channel Model

Consider a rate-8/9 coded partial-response (PR) channel illustrated in Fig. 1, where a block of 3640 message bits $x_k \in \{0, 1\}$ is encoded by a regular $(j, k) = (3, 27)$ low-density parity-check (LDPC) code [10], resulting in a coded block length of 4095 bits $a_k \in \{\pm 1\}$ with bit period T. The parity-check matrix has 3 ones in each column and 27 ones in each row. The readback signal can then be expressed as

$$p(t) = \sum\nolimits_k r_k q(t - kT) + n(t) + u(t), \qquad (1)$$

where $r_k = a_k * h_k \in \{0, \pm 2, \pm 4\}$ is the noiseless channel output, $*$ is the convolution operator, $q(t) = \sin(\pi t/T)/(\pi t/T)$ is an ideal zero-excess-bandwidth Nyquist pulse, $n(t)$ an additive white Gaussian noise (AWGN) with two-sided power spectral density $N_0/2$, and $u(t)$ is a TA signal.

A widely used TA model described by Stupp *et al.* [1] is considered in this paper as shown in Fig. 2, because it fits captured spin stand data and drive data very well [4]. This TA signal has a short rise time with a long decay time, and its effect is assumed to decay exponentially, which can be modeled as

$$u(t) = \begin{cases} A_0 t / T_r, & 0 \le t \le T_r \\ A_0 \exp\left(-(t - T_r)/T_d\right), & T_r < t \le T_f \end{cases} \qquad (2)$$

where $A_0 = \beta \sum_k |h_k|$ is the peak TA amplitude, $\beta \ge 0$ is the peak-factor, T_r is a rise time, and T_d is a decay constant. In this paper, the TA duration is assumed to be $T_f = T_r + 4T_d$ [5], where a decay time of $4T_d$ is sufficient because it will reduce the amplitude of the TA signal to approximately 1.8% of its peak amplitude.

At the receiver, the readback signal $p(t)$ is filtered by an ideal low-pass filter (LPF), whose impulse response is $q(t)/T$, to eliminate out-of-band noise, and is then sampled at a symbol rate of 500 Mbps [5], assuming perfect synchronization. The sampler output, y_k, is fed to the TA detection/correction block to obtain the corrected readback signal, z_k.

In a conventional setting, the TA detection/correction block is followed by a turbo equalizer, which iteratively exchanges soft information between the soft-output Viterbi algorithm (SOVA) [11] equalizer for the PR2 channel and the LDPC decoder (implemented based on the message-passing algorithm [11] with $N_{in} = 3$ internal iterations) for the outer code.

III. Existing TA Suppression Method

This paper focuses only on two TA suppression methods (i.e., one is based on a threshold-based technique, and the other is based on an LS fitting technique) because of its simplicity. We briefly explain how the two methods operate as follows:

A. Based on a Threshold-Based Technique

We denote the TA suppression method based on a threshold-based technique [5] as "**M1**," where the TA detection method is performed by first finding the average value of the readback signal, q_k, according to

$$q_k = \frac{1}{L} \sum_{i=k-\alpha}^{k+\alpha} y_i \qquad (3)$$

where y_i is the i-th sample of the readback signal, α is an integer, and $L = 2\alpha + 1$ is the window length for computing q_k. Then, a TA is detected if $q_k \ge n_1$ and $y_i \ge n_2$ for a few consecutive samples, where n_1 *and* n_2 are threshold values.

After the TA is detected, the TA detection operation is disabled and the TA correction operation is activated for a

duration of T_f. Then, the TA-unaffected readback signal, z_k, is obtained by subtracting the reconstructed TA signal from the TA-affected readback signal according to

$$z_k = \begin{cases} y_k - q_k, & \text{if TA is present} \\ y_k, & \text{if TA is absent} \end{cases} \quad (4)$$

B. Based on a Least-Squares Fitting Technique

Again, we denote the TA suppression method based on the LS fitting technique [6] as "**M2**." To detect a TA, we first find the averaged readback signal, q_k, from (3). Then, the TA is detected if only $q_k \geq n_1$.

After the TA is detected, the TA detection operation is disabled and the TA correction operation is activated for a duration of T_f so as to construct the estimated TA signal, $\hat{u}(t)$, based on the LS fitting technique and the samples $\{q_k\}$ [6]. This can be achieved by estimating the TA signal during a rise time and a decay time, where the TA signal during a rise time is approximately linear, whereas that during a decay time is exponentially decay [1]. Hence, the corrected readback signal is obtained from (4) by replacing q_k by $\hat{u}_k$, where $\hat{u}_k = \hat{u}(kT)$ is the k-th estimated TA sample.

IV. Iterative TA Suppression Method

A conventional receiver sends a sequence $\{z_k\}$ directly to the turbo equalizer. Specifically, the TA suppression method ignores the presence of ECCs, and is thus doomed to fail when the SNR is low enough. To solve this problem, the iterative TA suppression method was proposed in [7], where the TA detection/correction block, the SOVA equalizer, and the LDPC decoder exchange information as shown in Fig. 1. This paper investigates the performance of the two iterative TA suppression methods, one is based on M1 and the other is based on M2.

Denote the first time that the SISO decoder outputs the soft information λ_k as the *first* iteration. Clearly, the iterative scheme performs the same operations as the conventional receiver does at the first iteration. Nevertheless, after the first iteration, the soft information λ_k is fed back to both the SOVA equalizer and the TA detection/correction block. Then, an improved set of samples $\{z_k\}$ can be obtained by running the TA suppression method again, but this time it is performed on a sequence $\{c_k\}$, where $c_k = y_k - \tilde{r}_k$, $\tilde{r}_k = E[r_k|\lambda_k]$ is the k-th soft decision of r_k, and $E[\cdot]$ is the expectation operator. It can be shown that for a PR2 channel, the soft decision is given by [7]

$$\tilde{r}_k = \frac{A + B + C}{2\cosh(\lambda_k/2)\cosh(\lambda_{k-1}/2)\cosh(\lambda_{k-2}/2)} \quad (5)$$

where $A = 2\sinh((\lambda_k + \lambda_{k-1} + \lambda_{k-2})/2)$, $B = \sinh((\lambda_k + \lambda_{k-1} - \lambda_{k-2})/2)$, and $C = \sinh((-\lambda_k + \lambda_{k-1} + \lambda_{k-2})/2)$. Consequently, the improved samples $\{z_k\}$ are fed to the turbo equalizer, which generally yields an improved set of soft decisions $\{\tilde{r}_k\}$. The process repeats as many turbo iterations as required. It is evident that the turbo equalizer benefits from better samples $\{z_k\}$, and the TA suppression method benefits from better decisions $\{\tilde{r}_k\}$.

Table 1: The total number of operations (per bit) of each function.

Module	Number of operations (per bit)	
	Addition	Multiplication
SOVA	$7Q + \frac{\delta^2+9\delta+9}{2} + 1$	$6Q + 1$
LDPC decoder	$(1 + (k-1)(1-R))N_{in} + 1$	$(1-R)N_{in}$
Data exchange	2	0
Soft decision	8	9
M1	$(L-1) + T_f/P + C$	1
M2	$\{(L-1)P + 14T_d + 5T_r + T_f - 11\}/P + C$	$\{P + 18T_d + 2T_r + 11\}/P$

Table 2: Complexity (per bit) of different iterative TA suppression methods.

System	Number of operations (per bit)	
	Addition	Multiplication
Conventional receiver with M1	$50.251 + 222.17N$	$1 + 25.333N$
Iterative TA with M1	$(280.42 + C)N$	$35.333N$
Iterative TA with M2	$(283.87 + C)N$	$39.744N$

V. Complexity Comparison

To measure the complexity of iterative schemes, we consider the total number of additions and multiplications (per bit) as a criterion. Table 1 shows the complexity of each component, where $Q = 2^\nu$ is the number of trellis states [12]; ν is the target memory; δ is the decoding depth used in SOVA [11]; k is a parameter of an LDPC code [10]; N_{in} is the internal iterations used in the LDPC decoder; R is a code rate; P is the number of bits per sector, C is an indicator such that $C = 0$ if $N = 1$, and $C = 1$ if $N > 1$, and N is the number of turbo iteration. For a coded PR2 channel, the complexity of each iterative TA suppression methods is given in Table 2, where $\nu = 2$, $Q = 4$, $L = 51$, $\delta = 15$, $N_{in} = 3$, $k = 9$, $T_d = 1000T$, $T_r = 30T$, $T_f = 1030T$, $R = 8/9$, and $P = 4095$ bits.

It is of interest to compare the performance of different TA suppression methods when they have same complexity. Since multiplication has much more complexity than addition in terms of circuit implementation, we consider only the number of multiplications when comparing performances. Suppose that current technology can support the total number of multiplications equal to 10 iterations of the iterative TA suppression method with M2. It is clear from Table 2 that 10 iterations of the iterative TA suppression method with M2 are approximately equal to 11 iterations of that with M1, and 14 iterations of the conventional receiver (which utilizes the M1 to mitigate the TA effect at the first iteration only).

VI. Numerical Result

In simulation, every 4095-bit data sector is corrupted by one TA at the 500-th bit with $\beta = 2$, $T_r = 60$ ns, and $T_d = 0.5$ μs (i.e., a TA event $T_f = 1030T$) [5]. We compute the BER based on a minimum number of 10000 data sectors and 1000 error bits, and call that number as "BER given TA." For the PR2 channel, L = 51, $n_1 = 2.8$, and $n_2 = 4.5$ are suitable parameters for TA detection [6, 7].

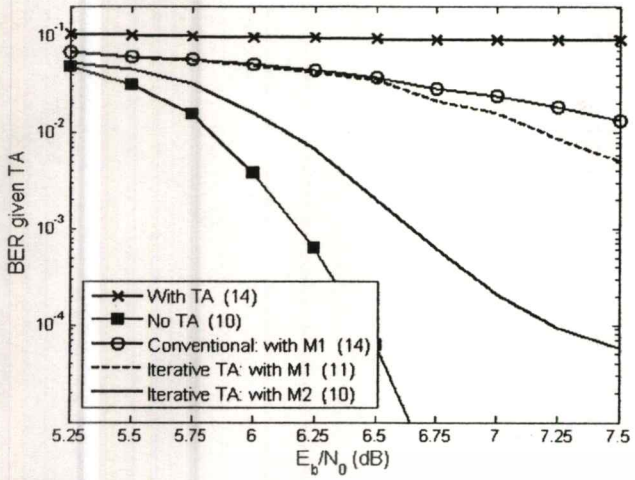

Fig. 3. Performance comparison of different schemes with same complexity.

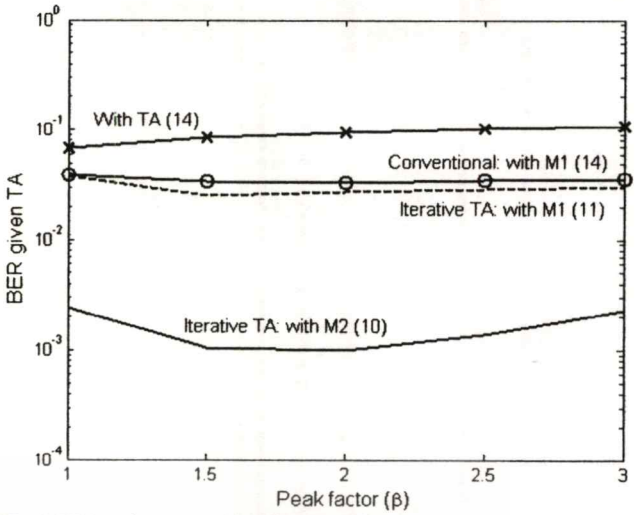

Fig. 4. BER performance with different peak factors.

Fig. 3 compares the performance of different schemes when they have *same* complexity, where the number inside the parenthesis indicates the number of iterations used to generate each curve, and the system performance in the absence of TA is referred to as "No TA." It is obvious that without the TA suppression method, the system performance is unacceptable, denoted as "With TA." As depicted in Fig. 3, the iterative TA suppression method with M2 outperforms that with M1 and the conventional receiver.

We also compare the performance of different schemes as a function of peak factors in Fig. 4. As expected, with same complexity, the iterative TA suppression method with M2 still outperforms that with M1 and the conventional receiver for all peak factors. This might be because the TA suppression method based on the LS fitting technique (i.e., M2) performs better than that based on the threshold-based technique (i.e., M1) as studied in [6].

VII. Conclusion

The TA effect can distort the readback signal to the extent of causing a sector read failure. Clearly, an iterative TA suppression method, which performs TA suppression and turbo equalization jointly, outperforms a conventional receiver with separate TA suppression and turbo equalization, especially when SNR is low. This paper investigates the performance of two iterative TA suppression methods based on the threshold-based technique (i.e., M1) and the LS fitting technique (i.e., M2).

Although M2 has more complexity than M1, it turns out that when the complexity is limited to a low-to-moderate amount, the iterative TA suppression method using M2 performs better than that using M1 and the conventional receiver. Thus, the iterative TA suppression method using M2 is more attractive for applications with strict complexity constraints.

Acknowledgment

This project is financially supported by a research grant CPN-R&D 01-23-52 EF from the Industry/University Cooperative Research Center (I/UCRC) in HDD Component, the Faculty of Engineering, Khon Kaen University and National Electronics and Computer Technology Center (NECTEC), National Science and Technology Development Agency (NSTDA), Thailand.

References

[1] S. E. Stupp, M. A. Baldwinson, P. McEwen, T. M. Crawford, and C. T. Roger, "Thermal asperity trends," *IEEE Trans. Magn.*, vol. 35, no. 2, pp. 752 – 757, March 1999.

[2] K. B. Klaassen and J. C. L. van Peppen, "Electronic abatement of thermal interference in (G)MR head output signals," *IEEE Trans. Magn.*, vol. 33, pp. 2611 – 2616, September 1997.

[3] V. Dorfman and J. K. Wolf, "A method for reducing the effects of thermal asperities," *IEEE J. Selected Areas Commun.*, vol. 19, no. 4, pp. 662 – 667, April 2001.

[4] M. F. Erden and E. M. Kurtas, "Thermal asperity detection and cancellation in perpendicular recording systems," *IEEE Trans. Magn.*, vol. 40, no. 3, pp. 1732 – 1737, May 2004.

[5] G. Mathew and I. Tjhia, "Thermal asperity suppression in perpendicular recording channels," *IEEE Trans. Magn.*, vol. 41, no. 10, pp. 2878 – 2880, October 2005.

[6] P. Kovintavewat and S. Koonkarnkhai, "Thermal asperity suppression based on least squares fitting in perpendicular magnetic recording systems," *J. of Applied Physics*, vol. 105, no. 7, 07C114, March 2009.

[7] P. Kovintavewat and S. Koonkarnkhai, "Joint TA suppression and turbo equalization for coded partial response channels," to appear in *IEEE Trans. Magn.*, 2010.

[8] S. B. Wicker, *Error control systems for digital communication and storage*. Upper Saddle River, New Jersey: Printice Hall International, 1995.

[9] T. Souvignier, A. Friedmann, M. Oberg, P. Siegel, R. Swanson, and J. Wolf, "Turbo decoding for PR4: parallel vs. serial concatenation," in *Proc. of ICC'99*, vol. 3, pp. 1638-1642, 1999.

[10] R. Gallager, "Low-density parity-check codes," *IRE Trans. on Inform. Theory*, vol. IT-8, pp. 21-28, January 1962.

[11] J. Hagenauer and P. Hoeher, "A Viterbi algorithm with soft-decision outputs and its applications," in *Proc. of Globecom'89*, pp. 1680 – 1686, November 1989.

[12] G. D. Forney, "Maximum-likelihood sequence estimation of digital sequences in the presence of intersymbol interference," *IEEE Trans. Inform. Theory*, vol. IT-18, no. 3, pp. 363 – 378, May 1972.

Author Biography

Personal Information

Name & Surname:	Mr. Theerachat Thongkam
Nationality:	Thai
Birth of date:	September 27th, 1975
Place of birth:	Ubonratchathanee, Thailand

Education

Bachelor degree

Field:	Electrical Engineering
Duration:	1995 - 1998
Institute:	Department of Industrial Electric Technology, Faculty of Engineering King Mongkut's University of Technology North Bangkok, Thailand

Master degree

Field:	Data Storage Technology
Duration:	2008 - 2013
Institute:	College of Data Storage Innovation, Faculty of Engineering, King Mongkut's Institute of Technology, Ladkrabang, Thailand

Research Interests

Themal asperity (TA) detect and suppression method, Low density parity check code, Hard disk drive technology, Read channel in Hard disk drive.

List of International Conference and Proceeding Papers

1. Chalit Chusin , Chutima Prasartkaew and, Somsak Choomchuay, "Non-Prime Parameters of LDPC Codes with Symmetrical Sub-matrix", ITC-CSCC, July 4-7, 2010, Pattaya, Thailand.
2. Chalit Chusin , Chutima Prasartkaew and, Somsak Choomchuay, "A Design of Non-prime LDPC Based on Interleave Modified Array Codes", DST-CON, July 30 – August 1, 2010, Bangkok, Thailand.
3. Chalit Chusin, Chutima Prasartkaew, Sekson Timakul, and Somsak Choomchuay, "A Design of Nonprime Block Irregular LDPC Codes via CRT", ISCIT 2010, October 26-29, 2010, Tokyo, Japan.